OPTIMIZATION OF A HIGH-THROUGHPUT 3D CELL CULTURING SYSTEM

[§]*Sing, D C; [§]*Rajendran, V G; [§]*Figueroa, E R; [§]*Bertucci, C P; [§]*Rosenthal, J A; *Stark, D J; **Filgueira, C S; *Raphael, R M; **Souza, G R
**Nano3D Biosciences, Inc. Houston, TX
*Bioengineering Department, Rice University, Houston, TX
[§]Equal Contribution
info@n3dbio.com

Objective: To optimize a device for 3D tissue culture along with Nano3D's magnetic levitation technology to achieve high-throughput functionality.

Methods: In order to create a practical and effective device that can facilitate 3D cell culture using magnetic levitation, certain criteria such as convenience of use, data quality, reusability, versatility, compatibility, and levitation yield must be established. Here, we examine these criteria and quantitatively evaluate prototype models of our device.

Results: Various proposed prototypes were evaluated through a Pugh matrix analysis. The scoring schemes for this assessment were derived from the established design criteria and experimentally tested. Various designs showed different weaknesses and strengths which are dependent on the desired application. While there are differences between the designs, such as adaptability and lack of co-culturing capability, the ability to control magnetic fields outweighs these disadvantages. Furthermore, additional accessories may be used to address any weaknesses in the various prototypes.

Conclusions: The prototype designs presented here are able to facilitate a smooth transition from existing high-throughput technology while maintaining functionality and providing increased effectiveness for 3D cell culture. The presented device offers scientists and researchers a novel high-throughput tissue culture method superior to traditional monolayer techniques. Overall, the technology has ground breaking application in drug development, therapeutic tissue regeneration, and pharmokinetic modeling.

PEO-MODFIIED SILICONES WITH ENHANCED BLOOD PROTEIN RESISTANCES

+Giese, M.L.; Bailey, B.M.; Grunlan, M.A.
+Texas A&M University; Department of Biomedical Engineering, College Station, TX
gies67@neo.tamu.edu

Objective: Adsorption of blood proteins by blood-contacting materials induces thrombosis which compromises device success and safety. Silicones have been utilized in many biomedical applications because of their excellent bulk properties including thermal and oxidative stability, gas permeability, low modulus, flexibility, and good biocompatibility. However, silicones generally exhibit poor resistance to plasma proteins because of its extreme hydrophobicity. To reduce protein adsorption, silicone surfaces have been hydrophilized by various approaches involving physical or chemical treatments or a combination of both. In contrast, poly(ethylene oxide) (PEO; or poly(ethylene glycol) PEG) is a neutral, hydrophilic polymer which exhibits unusually high protein resistance because of its hydrophilicity and configurational mobility. Thus, incorporation of PEO into silicones may improve the latter's protein resistance. In this study, we have prepared PEO-modified silicones using novel linear and branched PEO-silanes with flexible siloxane tethers to enhance protein resistance. PEO-silanes with the basic formulas were prepared: α-$(EtO)_3Si(CH_2)_2$-oligodimethylsiloxane$_n$-block-[PEO_m-OCH_3] (*linear architecture*) and α-$(EtO)_3Si(CH_2)_2$-oligodimethyl-siloxane$_n$-block-[PEO_m-OCH_3]$_2$ (*branched architecture*) (Figure 1). Finally, each were crosslinked via phosphoric acid (H_3PO_4)-catalyzed sol-gel condensation with α,ω-bis(Si-OH)PDMS (**P**, M_n = 3000 g/mol) and their resistance to blood protein adsorption was related to PEO-silane structure.

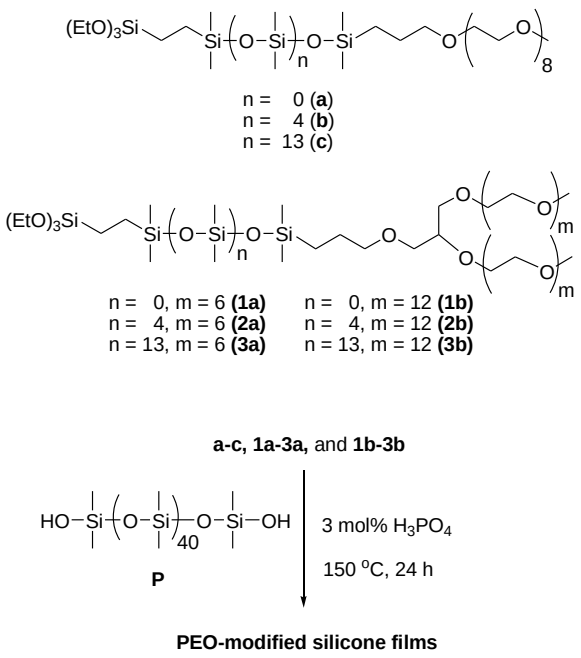

Figure 1. Linear and branched PEO-silanes with siloxane tethers. Each were reacted with silanol-terminated PDMS to form PEO-modified silicone films.

Methods: Linear PEO-silanes with the formula α-$(EtO)_3Si(CH_2)_2$-oligodimethylsiloxane$_n$-*block*-poly(ethylene oxide)$_8$-OCH_3 [n = 0 **(a)**, 4, **(b)** and 13 **(c)**] were prepared as previously reported.[1] Branched PEO-silanes with the formula α-$(EtO)_3Si(CH_2)_2$-oligodimethylsiloxane$_n$-*block*-[PEO_m-OCH_3]$_2$ where n = 0, m = 6 **(1a)**; n = 4, m = 6 **(2a)**; n = 13, m = 6 **(3a)** (i.e. the lower M_n PEO series) and n = 0, m = 12 **(1b)**; n = 4, m = 12 **(2b)**; n = 13, m = 12 **(3b)** (i.e. the higher M_n PEO series) were prepared as previously reported.[2,3] $(EtO)_3Si$-$(CH_2)_3$-$(OCH_2CH_2)_8$-OCH_3 served as the "PEO control" (i.e. no siloxane tether). Linear PEO-silanes **(a-c)** and branched PEO-silanes **(1a-3a** and **1b-3b)** were crosslinked to form PEO-modified silicone coatings.[1-3] AFM revealed significant surface reconstruction of the films when exposed to water.

Results: For PEO-modified crosslinked silicone films prepared with **a-c**, increased siloxane tether length produced surfaces with increased hydrophilicity, particularly after exposure to an aqueous environment, and enhanced protein resistance to bovine serum albumin (BSA). For PEO-modified crosslinked silicone films prepared with **1a-3a** and **1b-3b**, film surface hydrophilicity increased with siloxane tether length and decreased PEO M_n. All PEO-modified films adsorbed less BSA and human fibrinogen (HF) protein than the pure silicone control and resistance to protein adhesion generally increased with siloxane tether length. PEO M_n had an impact on protein adsorption behavior as well. For given siloxane tether length, less BSA adsorbed onto films based on the lower PEO M_n. Conversely, for given siloxane tether length, less HF adsorbed onto films based on the higher PEO M_n. AFM images revealed amphiphilic surfaces comprised of PEO domains in a silicone-enriched matrix. Surface features were dependent on siloxane tether length and PEO M_n.

Conclusion: For crosslinked PEO-modified silicone coatings, resistance to protein adsorption was enhanced with increased siloxane tether length of the PEO-silane. Enhancement in molecular mobility and amphiphilicity of the surfaces may contribute to this behavior.

References:

1. Murthy, R.; Cox, C. D.; Hahn, M. S.; Grunlan, M. A. *Biomacromolecules* **2007**, *8*, 3244-3252.
2. Bailey, B.M.; Murthy, R.; Grunlan, M.A. POLY Preprints (Amer. Chem. Soc., Div. Poly. Mater. Sci. Eng.), **2009**, *50(1)*, 535-536.
3. Murthy, R.; Bailey, B.M.; Valentin-Rodriguez, C.; Ivanisevic, A.; Grunlan, M.A**.** *submitted.*

IN VITRO BIODEGRADATION OF A NOVEL SEGMENTED POLY(ESTER URETHANE)

Ahmed Haque[1], David Dempsey[1], Robert S. Ward[2], Ananth V. Iyer[2], James P. Parakka[2], Elizabeth Cosgriff-Hernandez[1]*
[1]Biomedical Engineering, Texas A&M University, College Station, Texas
[2]DSM-PTG, Berkeley, California
Contact: ahaque89@tamu.edu

Objective: In tissue engineering, mammalian cells are seeded unto 3-D synthetic scaffolds serving as artificial extracellular matrices. Targeted use of biochemical cues and altered mechanical loads guide cellular differentiation and tissue regeneration. As long-term presence of the synthetic scaffold can be detrimental to regeneration and host compatibility, major emphasis is placed on the development of safe, biodegradable scaffolding. Increasingly, segmented polyurethanes (SPUs) appear a promising candidate for fulfilling such conditions. The characteristic tunability of SPUs allow for scaffolds with controlled degradation rates and biocompatible byproducts. Fundamental for the application of a given SPU is the need for detailed characterizations of its degradability. In this study, the degradation behavior of a novel bioresorbable poly (ester urethane) (PEsU) was observed at standard and accelerated rates of hydrolysis.

Methods: The study compared the bioresorbable PEsU against an observational control of a commercially available poly (ether urethane urea) (PEUU), BioSpan®; both were produced by DSM-Polymer Technology Group (Berkeley, CA, USA). Thirty-two strips of each SPU were divided into groups of four and immersed in solutions of phosphate buffered saline (PBS) and a 0.1M solution of sodium hydroxide (NaOH) for varying lengths of time. At one-week intervals, for four weeks, a group of strips of each SPU was removed from both solutions and observed for variations. Physical degradation was monitored by measuring each specimen's dimensions and mass prior to and following degradation periods. Fourier Transform Infrared Spectroscopy (FTIR) was used to observe qualitative differences in molecular structure of the samples. Changes in mechanical response transition temperature(s) were recorded using both dynamical mechanical analysis (DMA) and controlled temperature tensile testing. The DMA tests conducted were dynamic temperature ramps with a temperature range of -90°C to 80°C and a strain of 0.1% applied at a frequency of 1Hz. For tensile testing, mechanical response was recorded while specimens were deformed to 100% strain at a constant temperature of 37°C. Finally the specimen morphology was observed using scanning electron microscopy.

Results: As expected, the PEsU exhibited considerable signs of degradation as compared to the PEUU control. While additional results are still pending, current results show significant reductions in mass, thickness, and area of the PEsU strips. FTIR spectroscopy results reveal sharp declines in the $1730cm^{-1}$ peak of the PeSU spectra, corresponding to free carbonyls of the soft segment ester. These findings suggest the presence of both physical and bulk degradation. Results of the dynamic mechanical analysis and tensile testing show stronger mechanical responses to deformation following degradation likely due to the PEsU's increased ability to form perfect crystals. In contrast, little change in dimension, chemical composition, or mechanical response was observed in the PEUU.

Conclusions: This study confirms the hydrolytic degradability of the novel PEsU developed by DSM-Polymer Technology Group and suggests it as a potential candidate for future tissue engineering applications. As requirements for tissue engineering are variable and highly specific to application, further studies evaluating cell-material interaction, byproduct composition, and the feasibility of scaffold development have been proposed.

SHAPE MEMORY POLYMERS WITH SILICON-CONTAINING SEGMENTS

+Prukop, S.L.; Giese, M.L.; Zhang, D.; Weyand, C.B.; Grunlan, M.A.
+Texas A&M University, Department of Biomedical Engineering, College Station, TX
sprukop@gmail.com

Objective: Shape memory polymers (SMPs) are stimuli-responsive materials which have the ability to change shape upon application of an external stimulus such as heat.[1] SMPs, which exhibit transition temperatures tolerated by physiological tissues, large elastic deformation and also high moduli to withstand surrounding forces are desirable for interventional medical devices. Unique properties are often achieved by materials formed from a combination of inorganic, silicon-containing polymers with traditional organic polymers. In this research, we have prepared SMPs comprised of inorganic polydimethyl-siloxane (PDMS) and organic poly(ε-caprolactone) (PCL) segments. Networks were formed by the photochemical cure of diacrylated AcO-PCL_n-*block*-$PDMS_m$-*block*-PCL_n-AcO. In this system, PCL served as the switching segments and PDMS served as the soft segments to tailor mechanical properties. We demonstrate that mechanical and shape memory properties (e.g. shape fixity and shape recovery) can be systematically altered by changing the length of PCL and PDMS segments.

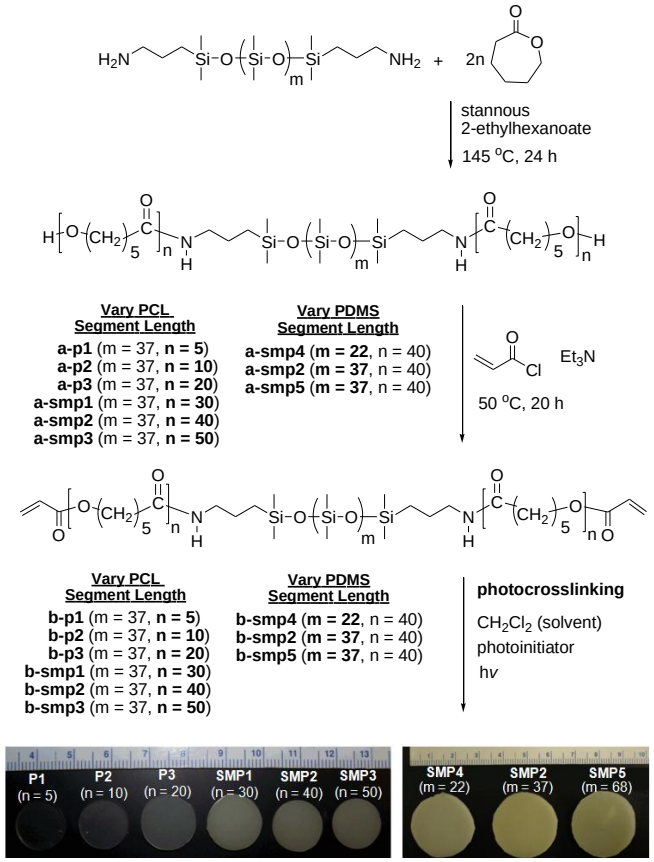

Figure 1. Synthesis and photochemical cure of AcO-PCL_n-*block*-$PDMS_m$-*block*-PCL_n-OAc macromers to form **P-1-3** and **SMP-1-5.** respectively. **SMP-1-5** exhibit shape memory behavior.

Methods: The HO-PCL_n-*block*-$PDMS_m$-*block*-PCL_n-OH macromers were prepared by ring-opening polymerization of ε-caprolactone in the presence of a tin catalyst and NH_2-$PDMS_m$-NH_2 by varying the molar ratio of NH_2-$PDMS_m$-NH_2 to ε-caprolactone. The terminal hydroxyl groups were subsequently converted to photosensitive acrylate (OAc) groups by subsequent reaction with acryloyl chloride to yield AcO-PCL_n-*block*-$PDMS_m$-*block*-PCL_n-OAc.[2] These acrylated macromers were each photochemically crosslinked to yield **P-1-3** and **SMP-1-5**. Macromers were dissolved in dichloromethane at various concentrations (25 and 50 wt %) and a photoinitiator consisting of 10 wt% solution of DMAP in NVP added. In a typical procedure, the macromer (3 g) was dissolved in CH_2Cl_2 (12 mL) and photoinitiator (1.8 mL) in a scintillation vial. After vortexing, this solution was transferred to circular silicone isolator wells (45 mm x 2 mm) sandwiched between two glass slides. This mold was then exposed to UV light (UV-Transilluminator, 6 mW/cm^2, 365 nm) for 3 min. The resulting solvent swollen discs were removed from the mold, air dried (RT, 12 h), and dried *in vacuo* (36" Hg, 80 °C, 4 h) to remove residual solvent. Uncrosslinked material was removed by soaking the disc in ethanol (~3 h), air drying overnight, and drying in vacuo as above. Using these specimens, thermal analysis by DSC, mechanical testing by tensile tests, and shape memory tests by DMA were conducted as previously described.[2]

Results and Conclusions: A series of new silicon-containing SMPs (**SMP-1-5**) was prepared via rapid photochemical cure of triblock macromers (AcO-PCL_n-*block*-$PDMS_m$-*block*-PCL_n-OAc). Thermal, mechanical, and shape memory properties of networks were systematically altered by the length of the PCL and PDMS segments. **SMP-1-5** exhibited shape memory behavior due to the ability of the PCL segments to effectively crystallize and act as switching segments. As PCL segment length increased and hence crosslink density decreased, an unusual simultaneous increase of *%ε*, *E* and *TS* was observed.

References:

1. Lendlein, A.; Kelch, S. *Angew. Chem. Int. Ed.*, 2002, **41**, 2034-2057.
2. Schoener, C.A.; Weyand, C.B.; Murthy, R.; Grunlan, M.A. *J. Mater. Chem. accepted.*

MANIPULATING BIO-PARTICLES BY AC ELECTRO-OSMOSIS

Jairo A Reyna, Nazmul Islam
University of Texas at Brownsville and Texas Southmost College
E-mail: Jairo.Reyna1@utb.edu, Nazmul.Islam@utb.edu

Objective: The purpose of this research is to study the separation of bio-particles by AC electro-osmosis (AC-EO). AC electro-osmosis is the fluid flow created by the non-uniform tangential component of the electric field produced by coplanar electrodes and the electrical double layer at the fluid-electrode interface. Small bio-particles of micro/nano size and latex particles will be subjected to AC-EO in order to study their separation.

Methods: Micro coplanar electrodes submerged under an electrolyte and subjected to AC voltage are used in order to create AC-EO. The microchips of coplanar gold electrodes are about 2 mm long, 160 micron wide and 120 nm thick separated by 20 microns in a micro-fluidic chamber (Figure a). The electrolyte, latex particles, and bio-particles (algae or bacteria) are placed in the chamber. Applying AC voltage creates the fluid flow and bio-particles travel from the edge of the electrodes to the surface of the electrodes where they are trap in the null point (Figure b). The bio-particles velocity will be recorded by using Moticam 2300 and Motic Image Plus software. The captured video will be analyzed frame by frame for characterization. Using a programmable LCR bridge HM18118 the impedance was analyzed in order to identify operating conditions of the ACEO produced by gold electrodes.

(a) 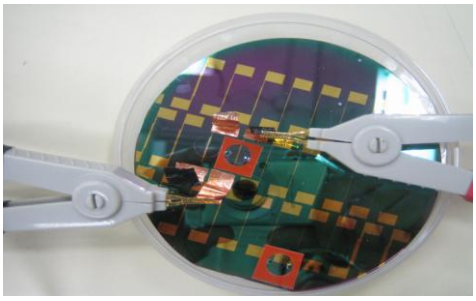 (b) 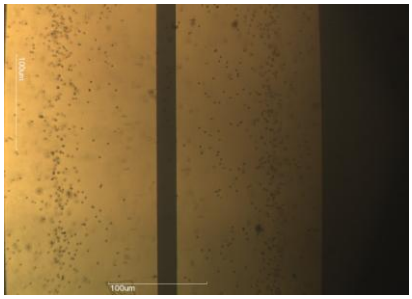

Figure: (a) Microchip Impedance experimentation; (b) Particles trapping at center of electrode

Results: The impediometric experiments served as a way to optimize the frequency, AC voltage requirements in which data is acquired. Preliminary experimental results using 1 micron latex particles are shown in Figure b. After applying the AC signal, suspended particles accumulate at the center of electrode from all directions. This is an ongoing experiment and data on bio-particle separation is being collected.

Conclusion: ACEO operate at relatively low voltages, which is suitable for integrated lab-on-a-chip systems. Bio-particle manipulation by ACEO mechanism may also be used as pre-processor in variety of bio-sensing applications.

DECOUPLING PEG HYDROGEL MESH SIZE AND MODULUS WITH THE INTEGRATION OF 4-ARM PEG

Thomas Wilems[1], Mary Beth Browning[1], Mariah Hahn[2], and Elizabeth Cosgriff-Hernandez[1]
[1]Biomedical Engineering, Texas A&M University, College Station, Texas
[2]Chemical Engineering, Texas A&M University, College Station, Texas
twilems@gmail.com

Objective: Bioactive hydrogels based on polyethylene glycol (PEG) coupled with collagen are of great interest in tissue engineering. PEG hydrogels intrinsically resist protein adsorption and cell adhesion. This provides a biological "blank slate" that can be used to carefully control cell-material interactions through the selective addition of bioactive molecules such as collagen. A range of hydrogel material properties are known to influence cell behavior in tissue engineered constructs, including modulus[1] and mesh size[2]. However, in order to increase the modulus of PEG-DA hydrogels, the mesh size is often sacrificed, which limits cell proliferation and viability. In order to determine the moduli and bioactivity levels that drive desired cell-material interactions, a hydrogel whose modulus and mesh size can be tuned in an uncoupled manner is needed. We hypothesized that the addition of an acrylated 4-arm PEG crosslinker would provide local increases in crosslink density which would increase gel modulus without significantly affecting overall permeability. In the current study, we report the effect of the 4-arm PEG crosslinker on modulus and mesh size of PEGDA-collagen hydrogels.

Methods: Linear and 4-arm poly(ethylene glycol) were acrylated using standard protocols. Briefly, the terminal hydroxyls were reacted with acryloyl chloride to form an ester linkage and acrylate end groups. The excess acryloyl chloride was neutralized, and the product was precipitated in cold diethyl ether. The structure was confirmed with NMR and FTIR spectroscopy.

Collagen Functionalization: Rat tail collagen type I (Sigma Aldrich) was functionalized with photoreactive crosslink sites to enable hydrogel formation.[3] Collagen was reacted with acrylate-PEG-N-Hydroxysuccinimide (ACRL-PEG-NHS, MW 3500, Jenkem Technology) in 50 mM sodium bicarbonate buffer (ph 8.5) at a molar ratio of 2:1 ACRL-PEG-NHS:NH_2 for 18 h. Excess ACRL-PEG-NHS and other reaction byproducts were removed via dialysis against 0.1 M HCl for 24 h and deionized water for 24 h (Slide-A-Lyzer, MWCO = 20,000, Pierce). Functionalization was confirmed with FTIR spectroscopy and SDS-Page.

Hydrogel Formation: A factorial design was used to determine the impact of PEG molecular weight (2000, 6000, and 10,000 g/mol), linear PEGDA concentration (10%, 20%, and 30%), and 4-arm PEG crosslinker concentration (0%, 10%, and 20%) on hydrogel modulus and mesh size. PEGDA hydrogel controls and PEGDA-collagen hydrogels were made with 1 mg/ml of functionalized collagen. A photoinitiator (Irgacure 2959, Sigma Aldrich) was added at a concentration of 10 mg/ml, and the solution was crosslinked into rings using a double walled cylindrical mold (ID=3 mm, OD=5 mm) via 10 min exposure to 365 nm UV light (Transilluminator, 9 mW/cm^2).

Hydrogel Characterization: After 24 hours of swelling in PBS, hydrogel rings were cut into slices (2-5 mm), and tensile testing to fracture was conducted at a uniaxial strain rate of 6 mm/min (Instron 3342). To determine the effect of hydrogel variables on mesh size, photoinitiated hydrogel plates (0.75 mm thick) were swollen in PBS for 24 hours. 8 mm diameter discs were soaked in 500µL of 50µg/ml dextran solutions for 24 hours. They were then transferred into a clean well plate with PBS for 24 hours. Two 150 µl aliquots were taken from each well and put into a 96 well plate. Fluorescence readings were taken at 480 nm of excitation and 520 nm of emission to determine the relationship between dextran hydrodynamic radius and diffusion into the hydrogel. This data was then used to provide a relative measure of hydrogel mesh size.

Results: *Synthesis:* An ester peak at 1704 cm^{-1} and loss of the hydroxyl peak at 3300 cm^{-1} in the FTIR spectra of PEGDA was indicative of successful acrylation. Proton NMR confirmed greater than 80% acrylation of all synthesized PEG diacrylates. FTIR spectroscopy also confirmed collagen functionalization as evidenced by an increase in the ether group peak at 1109 cm^{-1} with increased molar ratios of ACRL-PEG-NHS:NH2. SDS-Page displayed smearing of collagen bands in acrylated collagen due to decreased electrophoretic motility which further confirmed successful functionalization.

Hydrogel Characterization: A statistically significant increase in modulus was observed with increased concentration of 4-arm PEG crosslinker.

Conclusions: We have successfully demonstrated that the modulus of PEG hydrogels can be significantly increased with the addition of a 4-arm PEG crosslinker. The ability to adjust modulus while maintaining mesh size and permeability has significant impact in scaffold design.

References: [1] Bryant, et al. *Annals of Biomedical Engineering*, **32**, 407-417 (2004).
[2] Sebra, et al.. *Langmuir* **21**, 10907-10911 (2005).
[3] Engler, et al. *Methods in Cell Biology*, **83**, 521-545 (2007).

ENHANCEMENT OF AN IMPLANTABLE SELF-CLEANING THERMORESPONSIVE NANOCOMPOSITE HYDROGEL FOR BIOSENSORS

Alexander A. Abraham[1], Rebecca M. Gant[1], Ruochong Fei[1], Yaping Hou[1], Melissa A. Grunlan[1], and Gerard L Coté[1]
[1]Department of Biomedical Engineering, Texas A&M University, College Station, TX
aa.abraham@tamu.edu

Objective: The implantation of an optical biosensor will elicit an immune response involving protein and cellular adhesion that will eventually lead to fibrous encapsulation of the device, which may restrict analyte diffusion and impair the sensor's efficiency. In this research, a thermoresponsive nanocomposite hydrogel has been fashioned to compose a self-cleaning sensor membrane in an effort to diminish the host response.

Methods: The thermoresponsive nanocomposite hydrogel was assembled by the photopolymerization of an aqueous solution of *N*-isopropropylacrylamide (NIPAAm), *N*-vinylpyrrolidone (NVP), and polysiloxane colloidal nanoparticles. An *in vitro* study was administered utilizing GFP H2B 3T3 rat fibroblast cells. The experimental analysis examined the hydrogel's thermoresponsivity, glucose diffusion, and assessed cellular adhesion during its thermo-cycling over a 7 day time period. The hydrogel's thermoresponse was tuned by the introduction of a comonomer (NVP) to exhibit a maximum change in its swelling ratio around 39°C or near body temperature. Thermal cycling was used to initiate hydrogel swelling and deswelling and a concomitant alteration in surface hydrophilicity to promote cellular release.

Results: It was ascertained that the hydrogel significantly limited the degree of fibroblast adhesion as opposed to the polystyrene control.

Conclusion: Ultimately, this hydrogel may be utilized to govern biofouling *in vivo*.

INCORPORATION OF COLLAGEN-MIMETIC PROTEINS INTO BIOACTIVE HYDROGELS

M.B. Browning[1], T. Wilems[1], J. Rivera[2], B. Russell[2], M. Höök[2], D. Munoz-Pinto[3], M. Hahn[3], E. Cosgriff-Hernandez[1]
[1]Biomedical Engineering and [3]Chemical Engineering, Texas A&M University, College Station, Texas
[2]Institute for Biosciences and Technology, Texas A&M University System Health Science Center, Houston, Texas
mbrowning28@gmail.com

Objective: Tissue engineered vascular grafts (TEVGs) have the potential to restore function when conventional grafts are unavailable or fail. Although there have been significant advances in TEVGs, several obstacles still remain before they can be considered viable clinical alternatives. Past research has included the use of collagen-based hydrogels to aid in tissue repair. However, collagen's multitude of receptor binding motifs increases the risk of thrombosis and requires pre-seeding with endothelial cells prior to use. This study introduces the use of a Streptococcal collagen-like protein Scl2.28, termed Designer Collagens (DCs). This protein forms a triple helix similar to collagen but lacks collagen's numerous receptor binding motifs and risk of thrombosis. This provides a biological blank slate that can then be used to insert specific integrin binding sites using site-directed mutagenesis of the DC protein. Although DCs show great promise in cardiovascular applications, their use was previously limited due to the low mechanical properties of the protein and potential coating destabilization in physiological conditions. To address this limitation, we have developed a synthetic methodology to functionalize DCs with photocrosslinking sites to enable incorporation into a three dimensional hydrogel matrix. In this study, three DC proteins were functionalized with acrylate end groups for incorporation into poly(ethylene glycol) hydrogels. The DC proteins used are DC1, which has no receptor binding motifs, DC2, which has the integrin binding motifs $\alpha1\beta1$ and $\alpha2\beta1$, and DC3, which has the integrin binding motif $\alpha2\beta1$. Studies were then performed to confirm that functionalization did not disrupt the triple helix conformation and bioactivity.

Methods: *Synthesis:* Chemicals were purchased from Sigma-Aldrich (Milwaukee, WI, USA) and used as received. Acrylated PEG-(*N*-hydroxy succinimide) (NHS) was purchased from JenKem Technology (Beijing, China). PEG-DA was synthesized and purified according to the method developed by Hahn[1]. FTIR and NMR spectroscopy were used to verify end group functionalization. The DCs were functionalized via coupling lysine amino side groups with Acr-PEG-NHS(3500) according to the method developed by West[2]. FTIR spectroscopy and 10% SDS-PAGE gels were used to verify functionalization of DCs, and denaturing conditions were used to confirm the retention of the triple helix.
Integrin Binding: Recombinant integrin I-domains $\alpha1$ and $\alpha2$ binding to the functionalized DCs was determined using ELISA-type binding assays. Bound integrin was detected using anti-His HRP conjugate. Collagen type I was used as a positive control for integrin biding.

Results: *Synthesis:* Successful synthesis of PEG-DA and functionalized DC was verified with FTIR spectroscopy. Specifically, an absorption peak corresponding to the stretching vibration of an ester carbonyl (C=O) group not found in the spectrum of PEG diol was observed in the spectrum of PEG-DA at 1728 cm^{-1}. This is due to the esters introduced during functionalization. An absorption peak corresponding to the stretching vibration of an amide carbonyl (C=O) group not found in the PEG diol and PEG-DA spectra was observed in both the DC control and acrylated DC spectra at 1652 cm^{-1} due to the amides in the backbone of the proteins. In addition to FTIR spectroscopy, percent acrylation of the PEG was found using NMR analysis and was greater than 85% for all acrylations. Functionalization of the DCs was further confirmed using SDS-PAGE. Specifically, in the columns containing the functionalized DCs an upward smeared band can be seen in comparison to the control, indicating an increase in molecular weight with functionalization. Furthermore, SDS-PAGE confirmed the retention of the triple helix following functionalization. The functionalized Scl2s retained the ability to migrate as multimers on SDS-PAGE analysis, whereas heat denaturation resulted in monomers with molecular weights at ~ 35kd
Integrin Binding: Functionalization caused a modest decrease in integrin binding, but the reduction was not statistically significant.

Conclusions: We have successfully functionalized DC proteins with photocrosslinking sites for incorporation into 3D hydrogels matrices. The functionalization did not disrupt the triple helix conformation or integrin binding of the DC proteins. Current studies are investigating the effects of material variables on endothelial cell behavior. This research could potentially provide an increase in controlled bioactivity to tissue engineered vascular grafts.

References: [1] West JL. Advanced Materials 18, 2679-2684 (2006).
[2] Hahn M. Biomaterials

ALGINATE POROGEN DELIVERY SYSTEM FOR THE TREATMENT OF TRAUMATIC BONE DEFECTS

Buchanan, R.[a,b]; Murphy, M.[b]; Blashki, D.[b]; Fan, D.[b]; Yoon, D.[c]; Kasper, K.[c]; Liu, X.[b]; Jones, H.[d]; Noble, P.[d]; Weiner, B.[e]; Simmons, P.[b]; Mikos, A.[c]; Tasciotti, E.[b]; Ferrari, M.[a,b,c,f]

[a]The University of Texas at Austin, Austin, TX; [b]The University of Texas Health Science Center at Houston, Houston, TX; [c]Rice University, Houston, TX; [d]Barnhart Department at Baylor College of Medicine, Houston, TX; [e]The Methodist Hospital, Houston, TX; [f]The University of Texas M.D. Anderson Cancer Center, Houston, TX

Rachel.Buchanan@uth.tmc.edu

Objective: An extensive range of biocompatible and biodegradable polymeric scaffolds have been developed for bone tissue engineering applications. The porosity and pore interconnectivity of the scaffold is essential for tissue in-growth, vascularization and nutrient supply [1]. However, high porosity leads to compromised mechanical properties. Additionally, scaffolds are frequently pre-fabricated due to the heat produced during the crosslinking process. Poly (propylene fumarate) (PPF) addresses this issue through its ability to crosslink *in situ*. We therefore developed an *in situ* crosslinkable, injectable putty capable of providing mechanical stability to the bone lesion through the superior mechanical properties of PPF [2]. The use of an alginate porogen delivery system containing mesenchymal stem cells and bioactive molecules supplied the necessary components for enhanced tissue regeneration.

Methods: Alginate is a biodegradable polymer derived from seaweed that structurally resembles the glycosaminoglycan within the extracellular matrix making it a desirable environment for cell growth [3]. In this study, calcium alginate beads were fabricated and characterized to serve a dual purpose: 1) to create interconnected pores within a polymeric scaffold post-injection to invoke the infiltration of natural bone and 2) to encapsulate, protect and deliver the biological components essential for accelerating the regenerative process. The biological components delivered by the porogen were: mesenchymal stem cells, chemokines and mitogens contained in platelet-rich plasma and nanoporous silicon micro particles to provide sustained delivery of bioactive molecules that enhance stem cell activity at rates contingent upon the stage of fracture healing they compliment [4]. The alginate porogen was dispersed within the non cross-linked polymer prior to *in vivo* injection. Once injected, the physiological fluid dissolved the porogen thereby releasing the contents into the surrounding environment and creating a porous structure. The size of the alginate porogens as well as the PPF to porogen ratio was tailored to obtain the pore size and interconnectivity necessary for optimal tissue infiltration.

Results: Calcium alginate beads were successfully fabricated at the appropriate size of 200-500μm for optimal tissue integration *in vivo*. The rate of porogen degradation under simulated physiological conditions was characterized *in vitro*. The ability of the alginate porogen to encapsulate cells and maintain viability upon incorporation into the PPF matrix was confirmed as well as the preservation of growth factor bioactivity. Differentiation of stem cells within the scaffold was quantified using *in vitro* techniques. Mechanical testing using ASTM standards was performed on crosslinked scaffolds to determine whether the incorporation of alginate porogens provided temporary mechanical stability by filling the voids that would otherwise be present using pre-fabrication leaching.

Figure 1. 500μm alginate beads

Figure 2. Alginate dispersed in PPF (left) Pure PPF (right)

Conclusions: Through the use of alginate as a biocompatible and biodegradable porogen delivery system and the in vivo crosslinking abilities of PPF, a novel injectable scaffold is created that in every respect, is ideal for onsite care particularly in the case of traumatic fractures incurred during battle.

References: [1] Jones JR. New trends in bioactive scaffolds: The importance of nanostructure. *Journal of European Ceramic Society*. 2009; 9: 1275-1281

[2] Fisher JP, Dean D, Mikos AG. Photocrosslinking characteristics and mechanical properties of diethyl fumarate/poly(propylene fumarate) biomaterials. *Biomaterials.* 2002; 23(22): 4333-43

[3] Bhattarai N, Li Z. Edmondson D, Zhang M. Alginate-Based Nanofibrous Scaffolds: Structural, Mechanical, and Biological Properties. *Adv. Mater*. 2006; 18: 1463-1467

[4] Tasciotti E, Liu X, Bhavane R, Plant K, Leonard A, Price B, Cheng MC, Decuzzi P, Tour J, Robertson F and Ferrari M. Mesoporous Silicon Particles as a Multistage Delivery System for Imaging and Therapeutic Applications. *Nature Nanotechnology*. 2008; 3(3):151-157.

SWEET TOOTH MICELLES: SUGAR-RESPONSIVE ORGANOBORON BLOCK COPOLYMERS

Cambre, J N; Roy, D; *Sumerlin, B S
Southern Methodist University, Dallas, TX
bsumerlin@smu.edu

Objective: Segmented macromolecules with stimuli-responsive solution behavior are "smart" materials known as double hydrophilic block copolymers. Generally, these copolymers have an AB diblock structure in which one block (A) is hydrophilic and the other (B) can be hydrophobic or hydrophilic depending on the conditions of the surrounding environment. When an appropriate stimulus is applied, the block copolymers self-assemble into multimolecular aggregates with hydrophilic exteriors composed of the A block and hydrophobic regions composed of the responsive B block. Micelle or vesicle formation can be induced by changes in pH, temperature, and light. Our goal is to prepare block copolymers that respond to varying concentration of 1,2-diols (*e.g.*, glucose and fructose).
To accomplish this, we employ reversible addition-fragmentation chain transfer (RAFT) polymerization, because of its particular utility for the polymerization of monomers with sensitive functional groups.

Methods: Methods utilized have been previously reported (Cambre J N J. Am. Chem. Soc. 2007:129:10348-10349; Roy D Chem. Commun. 2008:2477-2479; Roy D Chem. Commun. 2009:2106-2108).

Results: Block copolymerization of 3-acrylamidophenylboronic acid (APBA) or 4-pinacolatoborylstyrene (pBSt) with *N*,*N*,-dimethylacrylamide (DMA) leads to well-defined block copolymers capable of self-assembly (Cambre J N J. Am. Chem. Soc. 2007:129:10348-10349; Roy D Chem. Commun. 2008:2477-2479). These block copolymers are unique because they demonstrate both pH- *and* sugar-responsiveness, as a result of the robust chemistry of their Lewis acid moieties. The resulting block copolymers are fully soluble in water above the pK_a of the boronic acid moieties. Below this pH, aggregates are formed that contain boronic acid moieties in the hydrophobic cores. Not only are these block copolymers expected to demonstrate pH-responsive behavior, but also the ability of the boronic acids to reversibly bind with 1,2- and 1,3-diols should impart sugar-responsive behavior. Near the pK_a of the boronic acid block, the addition of glucose shifts the equilibrium from the neutral boronic acid form (1) to the anionic boronic acid forms (2 and 3) (Scheme 1). The boronic acid block becomes water-soluble, resulting in the disassembly of the aggregates. Dynamic light scattering (DLS) and UV-Vis spectroscopy confirm the aggregation and dissociation of the block copolymers in response to changes in pH and sugar concentration.

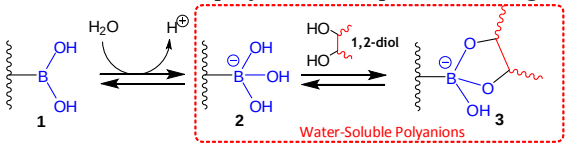

Scheme 1. Ionization and diol complexation equilibria of boronic acids in aqueous media

Chain extension of boronic acid containing polymers with *N*-isopropylacrylamide (NIPAM), a temperature-responsive polymer, leads to triply responsive block copolymers with the ability to form micelles or reverse micelles (Roy D Chem. Commun. 2009:2106-2108). This series of boronic acid block copolymers exhibit pH-, sugar-, and temperature-responsive behavior. Reversibility of the micelles was examined under varying pH and temperature conditions using variable temperature NMR spectroscopy and DLS.

Conclusions: By capitalizing on these unique responses, we aim to prepare nanomaterials with potential controlled release ability such that therapeutics (*e.g.*, insulin) can be automatically delivered when high glucose concentrations are detected. These materials have the potential to serve as "smart" insulin. This approach could combine the blood sugar monitoring and insulin delivery aspects of diabetes therapy.

PHOTOLITHOGRAPHICALLY AND SOFTLITHOGRAPHICALLY MICROFABRICATED POLY(ETHYLENE GLYCOL) HYDROGELS

Michael Cuchiara,[1] Jordan Miller,[1] Theodore Chen,[1] Alicia Allen,[1] Raul Villarreal[1] and Jennifer L. West[1]
[1]Department of Bioengineering, Rice University, Houston, Texas

Objective: Fabrication of microfluidic, multicellular, bioactive hydrogel scaffolds holds the potential to improve diffusion limited mass transport and develop tissue like microarchitectures ex vivo. In this work poly(dimethysiloxane) (PDMS) and poly(ethylene glycol) diacrylate (PEGDA) are serially molded to form a perfusable PEGDA microfluidic network in a PDMS housing. Combination with photolithography has shown the ability to spatially pattern multiple cell types within the microfluidic hydrogel, with control over mass transport characteristics and with the ability for cells to form organized structures.

Methods: *Softlithographic Microchannel Fabrication*: Perfusable PEGDA microchannels were fabricated using multilayer replica molding. PDMS was molded to a patterned photoresist master to fabricate a housing with perfusion access ports. Next, the PDMS housing was overlaid with a second photoresist master for the microchannel architecture and geometry. PEGDA was then injected into the housing around the photoresist master and exposed to UV light to form a hydrogel encased within a PDMS housing. The PDMS/PEGDA microchannel device was then peeled from the photoresist master and conformally sealed to cover glass. *Photolithographic Hydrogel Structure Fabrication*: In combination with the multilayer softlithographically fabricated constructs, photolithography was applied in order to photo-pattern cell laden PEGDA microstructures with independent cell types in spatially distinct locations. PEGDA solutions containing either endothelial cells (HUVEC) or neural progenitor cells (MHP 36) were exposed through different photomasks to fabricate MHP 36 pillars embedded within a perfused microfluidic HUVEC hydrogel matrix. *Mass Transport Studies*: Acellular PDMS/PEG microfluidic devices were fabricated as stated above with 6kDa PEGDA and perfused with variable molecular weight solutes (Toluidine blue 305 Da, 3kDa and 10kDa dextran) at 600 ul/hr through a 250 um channel. Diffusion from the channel through the bulk was imaged as a function of perfusion time using a CCD camera attached to a dissecting microscope. *Spatial Temporal Cell Viability*: NIH 3T3 fibroblasts were encapsulated (11E6 cells/mL) within a 6kDa PEGDA microfluidic hydrogel. The system was perfused through a 250 um channel with DMEM supplemented with 10% FBS at 600 uL/hr. Spatio-temporal cell viability was assayed (Live/Dead stain; Invitrogen) as a function of rtdistance from the perfused microchannel (0-1500 um), culture time (0-72 h), and static vs. perfused systems. *Perfused Tubulogenic Co-Cultures*: A 4:1 co-culture of HUVEC:10T ½ cells (pericyte precursors) were labeled with Cytotracker Green and Red respectively, encapsulated within a MMP degradable PEGDA derivative (30E6 cells/ml) with 2 mM acryloyl-PEG-RGDS and replica molded to yield a 250 um channel. The co-culture was perfused at 600 ul/hr for 96 hr with endothelial growth (EGM-2, Lonza). Tubulogenic activity and interactions of the co-culture with the perfused channel were determined by perfusion of the channel with fluorescent BSA and imaged using confocal microscopy.

Results: *Hydrogel Microchannel Fabrication Outputs*

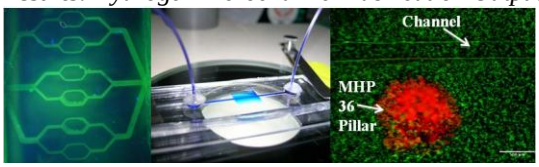

Figure 1. Replica molded PEGDA microfluidic network (left) perfused PDMS/PEGDA microfluidic device (center) and multilithographically fabricated hydrogel construct (Green=HUVEC, Red=MHP 36).

Spatial Temporal Mass Transport and Cell Viability Studies

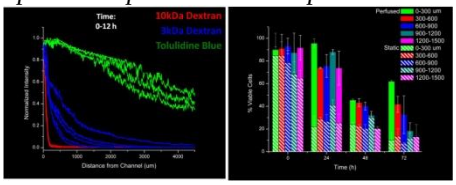

Figure 2. Spatial temporal diffusion plots for toluidine blue, 3 kDa & 10 kDa Dextran in 10% 6 kDa PEGDA (left). Spatial temporal cell viability of perfused (solid bar) and static (hashed bar) cultures (right).

Perfused Tubulogenic Co-Cultures

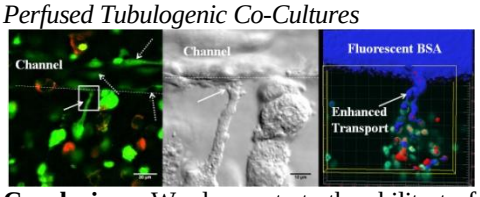

Figure 3. Cytotracker labeled co-cultures interacting with the perfused channel wall (left), phase image with increased magnification of HUVEC interaction with perfused channel wall (center) and perfusion of system with fluorescently labeled BSA shows enhanced transport at sites of tubulogenic activity.

Conclusions: We demonstrate the ability to fabricate perfusable microchannel networks and photo-pattern independent cell types within perfused PEGDA hydrogels. Enhanced mass transport within the perfused system provides spatio-temporal control over soluble - cell signaling interactions and maximizes cell viability. The ability to sustain tubulogenic co-cultures within the microfluidic hydrogel provides a tool to prevascularize scaffolds in vitro. Furthermore, enhanced mass transport observations within regions of high tubulogenic activity suggest potential anastomosis of tubules with the microchannel. Future research activities include evaluation of tubule structure interaction with perfused channels and fabrication of complex biomimetic multicellular tissue structures in vitro.

Acknowledgments: Funding support provided by NIH Biotechnology Training Grant and the NIH Quantum Grant.

MICROPATTERNING OF ELECTROSPUN POLYURETHANE FIBERS THROUGH CONTROL OF SURFACE TOPOGRAPHY

+Dempsey, D; +Schwartz, C; *Ward, R S; *Iyer, A V, *Parakka, J P; +Cosgriff-Hernandez, E
+Texas A&M University, College Station, TX
*DSM-PTG, Berkeley, CA
davedemp@tamu.edu

Objective: In recent years electrospinning has become a popular technique in tissue engineering primarily because of its ability produce scaffolds with interconnected pores for cell culture. The major limitation, however is that the pores produced are typically too small to promote favorable cell migration. In addition, basic electrospinning setups consisting of a flat plate collector will produce randomized fiber mats leaving the investigator little control over how cells will proliferate in the resultant scaffold. Previous research has focused on aligning fibers using collector setups such as a rotating mandrel or parallel plates. We propose a method to produce electrospun bioresorbable polyurethane fiber mats with patterns useful for tissue engineered vascular grafts by controlling surface topography of the fiber collector. In this study, soft lithography was used to control surface topography so that a bioresorbable segmented polyurethane could be patterned.

Methods: *Soft Lithography:* Sylgard 184 PDMS elastomer kit was used as received from The Dow Corning Company (Midland, MI, USA). Using a standard photolithography process, an SU-8 mold characterized by raised square patterns, 12µm high, of side lengths measured at 50, 100, 200, and 500µm was formed for the PDMS. A basic soft lithography process outlined by Xia was then used to make the PDMS replica.[1] The PDMS, mixed at a 10:1 base to curing agent ratio was spin coated on the SU-8 mold at 500rpm for 25 seconds to ensure a thin even layer of PDMS was coated on the mold. The elastomer was then cured in an oven set at 85°C for 20 minutes and peeled off when curing was completed. The resultant PDMS replica was expected to display features opposite that of the SU-8 mold. An optical profilometer was used to confirm the surface topography features on the PDMS collector substrates.
Electrospinning: BioSpan®, a commercially available poly(ether urethane)urea (PEUU), and an experimental bioresorbable poly(ester urethane) (PEsU) used in this study, were synthesized by DSM-PTG. N,N'-Dimethylacetamide (DMAC), was used as received from Sigma Aldrich (Milwaukee, WI, USA), to make 15 w/w% polymer solutions. The PDMS collector was attached to the front face of a copper plate positioned 20cm away from the tip of the blunted 23g1 syringe needle. The polymer solutions were dispensed at a rate of 0.2mL/hr as a voltage of 8.5kV was applied using a high voltage source purchased from Gamma High Voltage (Ormond Beach, FL, USA) for 3 hours. Morphology of the resultant fiber mats were observed with a scanning electron microscope.

Results: *Soft Lithography*: The successful fabrication of patterned PDMS collector substrates was verified with optical profilometry. Surface topography features consisting of 50, 100, 200, and 500µm grids were fabricated using soft lithography. Each grid pattern had raised grid lines approximately 20µm wide and 12µm high. The profilometer images also show consistent height among several features with little to no visible difference in height or width of the grid lines.
Electrospinning: Successful patterning of electrospun PEsU fibers was verified with scanning electron microscopy. Evidence suggests that the electrospun PEsU fibers mimic raised topography features on the collector substrate placed in front of the standard ground. Electrospun PEUU fibers however, were found to have no patterning effect thus showing that this phenomenon is potentially material specific.

Conclusions: We have successfully demonstrated a technique to pattern electrospun PEsU fibers. This technique is of particular interest in vascular tissue engineering due to its ability to potentially allow more control over compliance of the scaffold as well as the degradation profile and cell-scaffold interaction. Further investigation of the effect of fiber patterning on mechanical properties, degradation rate, and cellular alignment is currently in progress.

Reference: [1] Xia Y. Annu Rev. Mater. Sci. 1998; 28: 153-184

ENDOTHELIAL TUBE STABILIZATION AND SMC DIFFERENTIATION BY TGF-β1 LOADED PEGYLATED FIBRIN GELS

+Drinnan, C T; *Zhang, G; +Suggs, L J
+University of Texas at Austin, Austin, TX
*University of Akron, Akron, OH
c.drinnan@mail.utexas.edu

Objective: We have demonstrated that hMSC embedded within PEGylated fibrin gels without loaded or exogenous growth factors (GFs) demonstrate capillary tube morphology and endothelial cell (EC) phenotype. [1] However, capillary tube formation was not correlated to measured improvements in functional output with an acute MI model. [2] Smooth muscle cells (SMCs) stabilize neovascularization, and thus, a system that provides signals for SMC differentiation and maturation is desirable. Transforming growth factor-β1 (TGF) induces upregulation of late SMC markers from hMSCS, and stabilizes capillary tube formation. [3] We have previously loaded TGF into a fibrin gel PEGylated with a homobifunctional PEG. TGF maintained bioactivity and was sequestered within gels for at least 14 days. [4] The aim of the current study is to embed hMSCs into a TGF loaded PEGylated fibrin gel to induce EC and SMC differentiation. Further, multiple GFs can be loaded within the PEGylated fibrin gels via entrapment, conjugation, or physical affinity and released with varying kinetics if additional differentiation signals are required. [4]

Methods: Differentiation of hMSCs towards SMC has demonstrated a dependency on TGF concentration. [3] HMSCs (Lonza) were seeded at 2 k-cells/cm2 on tissue culture treated poly(styrene) (TCP) in media (Lonza) with TGF concentrations of 0, 0.1, 1, and 10 ng/ml for 1, 4, and 7 days. Media was changed at day 4. Reverse transcription qRT-PCR was performed with primers (ABI) against EC (VE-CAD, CD31, VEGF, vWF, CD13) and SMC markers (ANGPT1, ANGPT2, CAL, DES, SMA, PDGF-Rβ). β-actin was utilized as an endogenous control and RNA production was normalized to control hMSCs. Porcine Fib (Sigma) was PEGylated with PEG-(SCOP)2, 3400 MW (NOF America) at 1:10 molar ratio and reacted with human TGF (R&D Systems) for 30 min in PBS, pH 7.8 at 37ºC. HMSCs in media are mixed with GF loaded Fib solution. Crosslinking was initiated with human thrombin in 40 mM CaCl2 (Sigma). The final concentration of TGF was 25 ng/ml; Fib, 10 mg/ml; hMSCs, 50 kcells/ml; and thrombin, 12.5 U/ml. PBS was used in lieu of PEG or TGF as controls. Reverse transcription qRT-PCR and immunohistochemistry were performed at days 7 and 14.

Results: RNA production of hMSCS cultured on a monolayer was measured over 7 days. HMSCs demonstrated upregulation of SMA and CAL at day 7 compared to hMSCs at day 1. Further, 10 ng/ml TGF induced greater upregulation of CAL compared to unexposed cells. EC markers were downregulated at 10 ng/ml TGF concentration, which matches current literature. [3] Nevertheless, preliminary qRT-PCR data indicates that upregulation of SMC and EC phenotype occurs at day 14 in TGF loaded PEGylated fibrin gels.

Conclusions: HMSCs when exposed to TGF on TCP have demonstrated upregulation of SMC markers as quantified via qRT-PCR. Further, hMSCs embedded within loaded PEGylated fibrin gels demonstrate upregulation of EC and SMC markers.

References:

1. Zhang, G. and L.J. Suggs, *Vascular differentiation of bone marrow stem cells is directed by a tunable 3D matrix.* Acta Biomaterialia, In Review.
2. Zhang, G., et al., *Controlled Release of Stromal Cell Derived Factor-1alpha In situ Increases C-kit+ Cell Homing to the Infarcted Heart.* Tissue Engineering, 2007. **13**(8): p. 2063-2071.
3. Ross, J.J., et al., *Cytokine-induced differentiation of multipotent adult progenitor cells into functional smooth muscle cells.* J. Clin. Invest., 2006. **116**(12): p. 3139-3149.
4. Drinnan, C.T., et al., *Controlled release of transforming growth factor-beta1 and the BB isoform of platelet derived growth factor from PEGylated fibrin gels.* Journal of Controlled Release, In Review.

NANO-STRUCTURED SILICON/POLYMER COMPOSITE MICROSPHERES FOR SUSTAINED RELEASE OF BIOMOLECULES

Fan, D; De Rosa, E; Yadzi, I; Peng, Y; Smid, C; Liu, X; Ferrari, M; Tasciotti, E
University of Texas Health Science Center at Houston, TX
Dongmei.Fan@uth.tmc.edu

Objective: The sustained release of bioactive molecules can be achieved through the use of polymeric delivery systems. Poly (DL-latide-co-glycolide) (PLGA) particles for examples, provide controlled release yet, unfortunately, the acidic by-products of their degradation induce inflammatory responses (1) and affect the bioactivity of the loaded molecules (2). In this work we demonstrate that the use of biocompatible silicon nanoporous (NPSi) microparticles (MPs) (3) together with agarose coating prior PLGA encapsulation, represent valuable solutions to these disadvantages.

Methods: PLGA/NPSi microspheres were fabricated by a solid-in-oil-in-water emulsion method. Load and release of FITC-BSA was quantified by fluorimetry. Upon agarose coating, protein stability was tested by adding trypsin and monitoring protein digestion through polyacrylamide gel electrophoresis (SDS page), HPLC and MALDI analysis.

Results: We generated PLGA/NPSi microspheres encapsulating multiple silicon particles as shown by confocal microscopy (Figure 1). These composite microspheres provided sustained release of BSA for up to 30 days (Figure 2). NPSi/PLGA microspheres did not significantly alter physiologic pH and, when incubated with cells, were not internalized and did not induce any cytotoxic effect. Agarose coating provided protein protection without affecting particle degradation and protein release rates. As shown by SDS page (Figure 3), the BSA released from agarose coated MPs had less digestion products than the BSA released from the not coated MPs.

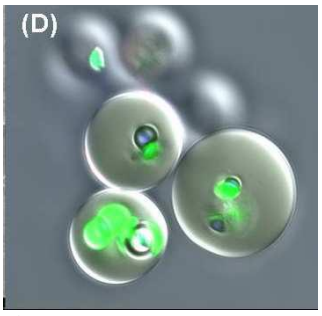

Figure 1

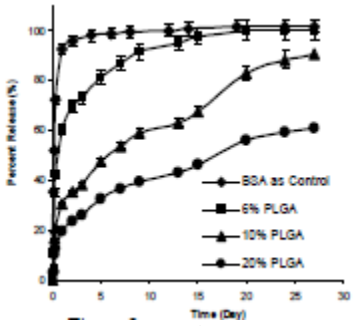

Figure 2

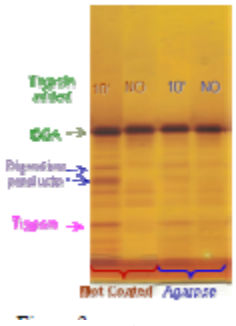

Figure 3

Conclusion: Successful sustained release of FITC-BSA for 30 days can be achieved by the NPSi/PLGA microspheres platform. Agarose coating is a valuable solution against protein instability during long term release. The combination of PLGA and agarose coatings represent an ideal solution to provide sustained and effective long term delivery of bioactive factors in tissue engineering application such as wound healing and bone tissue engineering.

References

1. M. Ara, Y. Imai. Biomaterials 23 (2002) 2479-2483.
2. M. Igartua, R. M. Hernandez, A. Esquisabel, A. R. Gascon, M. B. Calvo, J. L. Pedraz. International Jounal of Pharmaceutics 169 (1998) 45-54.
3.Tasciotti E, Liu X, Bhavane R, Plant K, Leonard A, Price B, Cheng MC, Decuzzi P, Tour J, Robertson F and Ferrari M. *Nature Nanotechnology* 3 (2008) 151-157.

THERMORESPONSIVE NANOCOMPOSITE DOUBLE NETWORK HYDROGELS AND THEIR CELL-RELEASING BEHAVIOR

+Fei, R; George, J.T.; Grunlan, M.A.
+Texas A&M University, College Station, TX
rfei@neo.tamu.edu

Objective: Crosslinked poly(*N*-isopropylacrylamide) (PNIPAAm) hydrogels undergo a reversible volume phase transition in water from a swollen to a deswollen state above their volume phase transition temperature (VPTT; ~33 °C). Thermal cycling of PNIPAAm hydrogels is useful for controlled detachment of cultured cells.[1] Extending the utility of PNIPAAm hydrogels as robust cell-releasing materials for implanted biosensor membranes requires improved mechanical properties and degree and rate of swelling/deswelling for better cell-release. Double-network (DN) hydrogels may exhibit exceptional strength.[2] A DN hydrogel is synthesized in two steps with the first hydrogel highly crosslinked and the second hydrogel loosely crosslinked. Also, incorporation of a nanoscale filler to create a nanocomposite may also increase hydrogel strength. In this study, we prepared thermoresponsive nanocomposite DN hydrogels based on PNIPAAm and polysiloxane nanoparticles (~ 54 nm).

Methods: Polysiloxane colloidal particles were prepared by cationic emulsion polymerization of D_4 and D_4^{Vi}.[3] The resulting nanoparticles were subsequently stabilized by crosslinking.[4] 10.4% (solid content). DLS: 54 nm (ave. diam.) and 0.2 (polydispersity, PD). DN hydrogels were prepared in two sequential steps. The 1st network was obtained by the photocure of aqueous precursor solutions containing NIPAAm monomer (1.0 g, 8.84 mmol), BIS crosslinker (0.02 g, 0.13 mmol), and Irgacure-2959 photoinitiator (0.08 g, 0.36 mmol) and DI water (the total volume equal to 7 mL including the volume of water introduced later by the nanoparticle emulsion). Finally, the appropriate amount of emulsion containing nanoparticles was added (Table 1). Hydrogel sheets (1.5 mm thick) were prepared by pipetting the solution between two clamped glass microscope slides (75 x 50 mm) separated by polycarbonate spacers. The mold was submerged in an ice water bath (~7 °C) and exposed to UV light (6 mW/cm^2, 365 nm) for 30 min. The hydrogel sheet was rinsed was soaked in DI water for 1 day with to remove impurities and then soaked in a solution of NIPAAm (6 g), Irgacure-2959 (0.24 g), BIS (0.012 g) and 7 mL DI water for 1 day at 7 °C. The hydrogel sheet was transferred to similar mold (2.3 mm thick) and likewise photocured.

Table 1. DN Hydrogel Compositions

	1st Network		2nd Network	
Notation	%BIS	%NP	%BIS	% NP
2% SN	2%	--	--	--
2% - 0.2%	2 %	--	0.2%	--
3% - 0.2%	3 %	--	0.2%	--
4% - 0.2%	4 %	--	0.2%	--
2%NP - 2% - 0.2%	2 %	2%	0.2%	--
2% NP - 3% -0.2%	3 %	2%	0.2%	--
2% NP - 4%- 0.2%	4 %	2%	0.2%	--

SN = single network (no 2nd network) BIS = wt% based on NIPAAm
% NP = (wt % solids of nanoparticles with respect to total precursor solution wt)

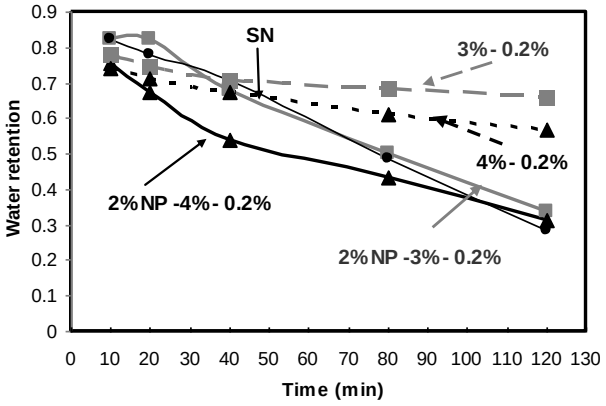

Figure 1. Deswelling kinetics

Results: Increasing the levels of BIS crosslinker in the 1st network systematically increased compressive storage modulus (TA Instruments Q800). For DN prepared with 3 and 4% BIS crosslinker in the 1st network, introduction of polysiloxane nanoparticles led to significant increase in the rate of deswelling (Figure 1).

Conclusions: Thermoresponsive DN hydrogels were prepared with polysiloxane nanoparticles. Because of their enhanced strength and deswelling kinetics, they may be particularly useful in applications requiring mechanical integrity and rapid cell-release such for biosensor membranes which self-clean in response to thermal modulation. Our group has previously shown that "single-network" nanocomposite hydrogels release cells with thermal modulation and such studies will be conducted for these.

References:
1. Yamato, M, et al. *Prog. Polym. Sci.*. 2007**, *32*, 1123.**
2. Tankaka, Y., et al. *Progr. Polym. Sci.* **2005**, *30*, 1.
3. Lin, M., et al. *J. Disp. Sci. Tech.* **2004**, *25*, 827.
4. Zhang, D., et al. *J. Appl. Poly. Sci.* **2003**, *89*, 3587.
5. Hou, Y., et al. *Biomaterials* **2008**, *29*, 3175.

BIOACTIVE HYDROGEL MICROSPHERES AS A VERSATILE SUPPORT AND DELIVERY SYSTEM FOR STEM CELL-BASED THERAPIES

+Franco, C L; West, J L
+Rice University Houston, TX
clfranco@rice.edu

Objective: Neural stem cells (NSCs) have shown significant promise for treating a variety of central nervous system disorders.1 For a therapeutic approach to be successful, however, the cells must be provided with both structural support and a favorable microenvironment. Mimicking the adult NSC niche, where proliferating neural precursors are observed near sites of angiogenesis, may be one solution.2 This research investigates the use of a biocompatible, bioactive poly(ethylene glycol) or PEG-based hydrogel as a biomimetic scaffold for neural stem cell-based therapy. The hydrogel material was covalently modified to present specific bioactive peptides and protease sensitive sequences for cell mediated degradation.3 Additionally, a method was developed to allow rapid microencapsulation of cells within this material while preserving high viability. The microsphere formulation was demonstrated to sustain complex cell interactions *in vitro* and could potentially allow injectable delivery of these prestarted tissue constructs for therapeutic applications.

Methods: Succinimidyl carboxymethyl PEG monoacrylate was covalently bound to the cell adhesive peptide, RGDS. Similar chemistry was utilized to embed a collagenase sensitive peptide, GGGPQGIWGQGK between two acrylated PEG spacers to form the backbone of the MMP-sensitive hydrogel. A 10% solution in PBS of this polymer was cross-linked into a hydrogel by addition of 100 μmole/mL Eosin Y photoinitiator, 3.4 μL/mL N-vinylpyrrolidone, 1.5% v/v triethanolamine and exposure to light from a metal halide lamp. Microspheres were produced by cross-linking the polymer solution after generation of an emulsion in sterile mineral oil containing 3 μL/mL 2-2-dimethoxy-2-phenyl acetophenone in N-vinylpyrrolidone (300 mg/mL). Control over cell behavior was demonstrated by evaluating the adhesion and spreading of NSCs on the surface of hydrogels containing varying concentrations of the RGDS adhesive peptide. Encapsulated cell viability was assessed with calcein AM and ethidium homodimer staining. Versatility of the polymer microspheres to support niche-like interactions was demonstrated with a conditionally immortalized neural stem cell line (MHP36) and an immortalized murine brain endothelial cell line (bEnd.3, ATCC). Potential for prevascularization was investigated with a co-culture of human umbilical vein endothelial cells (HUVEC, Lonza) and smooth muscle progenitor cells (10T1/2, ATCC). Immunostaining was performed to monitor these co-culture interactions within the particles over time.

Results: The microsphere encapsulation procedure was optimized to preserve high viability for multiple cell types. With *in vitro* culture, these hydrogel particles were observed to support long term survival, proliferation and spreading, of cells in a 3D environment. A 1 to 1 co-culture encapsulation of bEnd.3 and MHP36 cells developed extensive interactions between endothelial processes and proliferating NSC clusters which were similar to those observed in the *in vivo* niche.3 A co-culture system of HUVECs and 10T1/2 cells provides a more complex model of angiogenesis with which the NSCs can interact. DAPI and phalloidin staining was used to visualize a 4 to 1 co-culture microencapsulation of HUVEC and 10T1/2 cells. By 7 days the cells had organized into a primitive vascular plexus within the particles which was stable for over 14 days in culture.

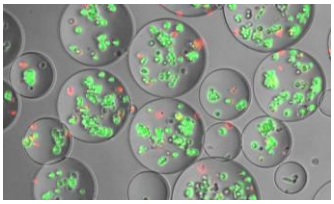

Figure 2. Overlay of brightfield and Calcien AM, ethidium homodimer viability staining of microencapsulated NSCs

Conclusions: This research introduces highly tunable, hydrogel microspheres as a platform technology for neural tissue engineering. The particles are demonstrated to support multiple cell types as well as complex co-cultures interactions *in vitro.* In addition to the RGDS peptide used here, the material can be precisely modified through the covalent attachment of multiple peptides or whole proteins in order to mimic the microenvironment of the *in vivo* niche. Providing an appropriate surrogate niche for implanted NSCs may be the key to promoting successful survival and engraftment with the host tissue. Finally, the microsphere formulation which can be achieved through a simple oil emulsion provides structural support to the cells while still allowing delivery via controlled injection.

References:

1. Lundberg C. Exp Neuro. 1997;145:342-360.
2. Palmer TD. J Comp Neurol. 2000;425:479-494.
3. West JL. Macromol. 1999;32:242-244.

GUIDED DIFFERENTIATION OF MOUSE EMBRYONIC STEM CELLS WITH PROTEIN-IMMOBILIZED BEADS

L. Geuss[1], G. Zhang[2], and L.J. Suggs[1]
[1]The University of Texas at Austin, Austin TX, [2]The University of Akron, Akron OH
lgeuss@mail.utexas.edu

Objective: The purpose of this project is to develop a system to guide differentiation of Mouse Embryonic Stem Cells (mESC) into cardiovascular progenitor cells. Pre-differentiation of ESCs prior to injection *in vivo* is required to prevent tumor formation.[1] The Sonic hedgehog (Shh) signaling cascade has been shown to drive differentiation of mouse ESCs (mESC) towards mesodermal progenitor fates.[2] Our group has demonstrated that aggregation of mESCs into embryoid bodies (EB) can direct differentiation into cardiovascular cell types.[3] In this study, we presented mESC in EBs with Shh-conjugated dynabeads to direct early mesodermal commitment of the mESCs.

Methods: R1 mESCs (A. Nagy, Toronto, Canada) were expanded in ES Knockout culture medium (Invitrogen) on inactivated Mouse Embryonic Fibroblast (MEF; ATCC) feeder layers as described previously.[3] Shh was purchased with a 6x histidine tag on the N-terminus (R&D Systems). The Shh protein was localized to dynabeads with an antibody against the histidine tag (Invitrogen) at various concentrations (1-10nM). The Shh-conjugated dynabeads were co-cultured with the mESC in Aggrewell plates (Stem Cell Technologies) without LIF supplementation for 72 hours to allow aggregation into EBs (**Figure 1**). Control groups were presented with soluble Shh in the culture medium. Immunohistochemistry and FACS analysis were used to analyze undifferentiated ESC markers (SSEA-1 and OCT-4).

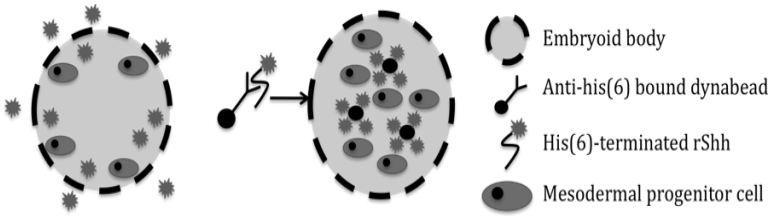

Figure 1: Model of Shh presentation to Embryoid Bodies. (A) Soluble Shh is restricted to the EB periphery. (B) Shh-bound dynabeads increased differentiation of ESC into mesodermal progenitor cells, and distribute uniformly.

Results and Discussion: Immunohistochemistry demonstrated that recombinant Shh was uniformly distributed within the core of the EB (**Figure 2**). Soluble Shh was only distributed to the periphery of the EB. This suggests that Shh can be presented to the interior of EBs using dynabeads, increasing the number of cells exposed to the protein. FACS analysis was used to calculate the number of cells positive for undifferentiated and differentiated markers. By day 12 in 2D culture, there was a relatively high concentration of cells positive for SSEA-1 (9.0%) and OCT-4 (39.5%). Only intermediate expression levels of markers for differentiated cell types (CD31, 4.0% and VE-cadherin, 14.9%) were calculated in comparison.

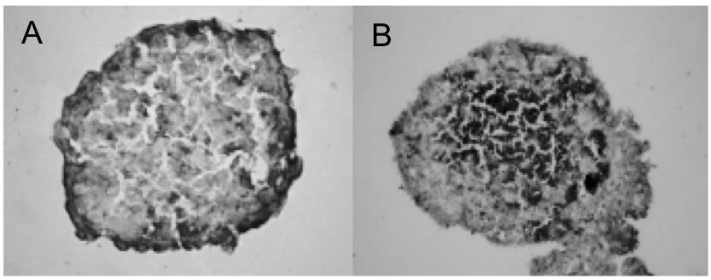

Figure 2: (A) localization of Shh to the outer, endodermal layer of the EB, 20X; (B) localization of Shh-immobilized proteins within the EB, 20X

Conclusions: Shh-immobilized beads support uniform Shh presentation to a higher concentration of cells within the EB compared to soluble Shh. FACS analysis demonstrates the potential of these cells to differentiate into mesodermal progenitor cells. This method for pre-differentiation allows us to yield high concentrations of mesodermal progenitor cells that can be used for *in vivo* repair of MI.

References:

[1]Saric T. Cells Tissues Organs. 2008; 188: 78-90
[2]Vokes S. Development. 2004; 131: 4371-4380
[3]Liu H. Biomaterials. 2006; 27: 6004-6014

COMBINATORIAL EFFECTS OF MATRIX ELASTICITY AND CELL SHAPE ON MESENCHYMAL STEM CELL DIFFERENTIATION

BJ Gill,[1,2] Stephanie Nemir,[1,2] and Jennifer L. West[1]
[1]Rice University, Houston, Texas USA
[2]Baylor College of Medicine, Houston, Texas USA

Objective: It has been shown that cells are able to sense and respond to their substrate microenvironment, affecting cell proliferation, migration, gene expression and stem cell differentiation[1]. In particular, lineage-specificity of human mesenchymal stem cells (hMSC) differentiation is dependent on substrate elasticity and size restrictions in cell shape[2,3]. Tuning these factors together will eliminate confounding between the two factors and may improve lineage-specific yields. Using a laser scanning lithography (LSL) technique we are able to surface-pattern restricted cell adhesive areas on poly(ethylene glycol)-diacrylate (PEGDA) hydrogels synthesized over a physiologically relevant range of stiffnesses and examine changes in hMSC differentiation with immunostaining for lineage-specific markers.

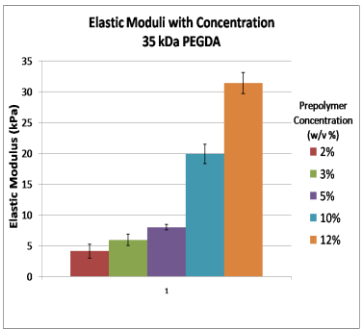

Figure 1: **Elastic Moduli of 35 kDa PEGDA Hydrogels**

Methods: Hydrogel preparation: PEGDA was synthesized by reacting 35 kDa PEG with acryloyl chloride in triethyl amine and dichloromethane overnight, purified with phase separation in a K_2CO_3 solution and precipitated in diethyl ether. Base hydrogels were prepared by photocrosslinking 35 kDa PEGDA using an acetophenone photoinitiator and 30 second UV exposure time. Polymer concentration was varied to form hydrogels of variable stiffness. Elastic moduli were determined via tensile testing. Surface Patterning: A polymer solution with 35 µmol/mL acryloyl-PEG-RGDS, 1 µmol/mL eosin Y, 1.5% triethanolamine and 4 µL/mL NVP was prepared. A 5 mm diameter hydrogel sample was placed on 10 µL droplet of this polymer solution in a #1 cover glass chamber plate. A Zeiss 5Live confocal microscope was focused on the polymer-gel interface and scanned across the sample in programmed region-of-interest (ROI) geometries. Unrestricted patterns with ROIs spanning the entire gel surface were first tested as controls. Cell Culture: hMSCs (Lonza) were seeded on patterned gels at 10,000 cells/cm^2 in MSC Basal Growth Media at passage numbers less than 6. Samples were taken through 3 cycles of osteogenic induction, adipogenic induction or control growth media changes over 12 days. Immunostaining: Samples were fixed, permeablized, blocked and stained for lineage-specific markers: Primary antibodies were targeted against adiponectin for adipogenic differentiation and osteocalcin for osteogenic differentiation. Samples were counterstained with DAPI and imaged on a Zeiss 5Live confocal microscope.

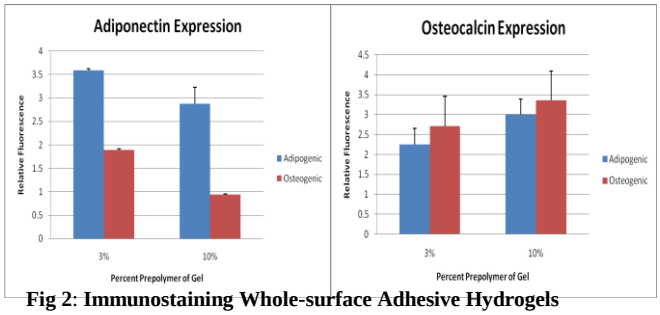

Fig 2: **Immunostaining Whole-surface Adhesive Hydrogels**

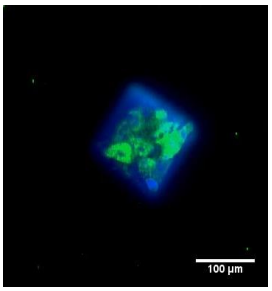

Figure 3: hMSCs on 100 µm Pattern
Adiponectin (Green) and DAPI (Blue).

Results: Elastic moduli were found for 35 kDa hydrogels at various prepolymer concentrations (Fig 1). For most cell studies 3% and 10% were used with moduli of 5.6 and 19.9 kPa, respectively. In non-size restricted controls, staining differences were most evident with adiponectin and osteocalcin markers (Fig 2). Adiponectin staining demonstrated highest adipogenic differentiation on softer substrates in adipogenic media and elevated differentiation on softer substrates despite culture in osteogenic media. Osteocalcin staining showed a similar trend with highest osteogenic expression on stiffer substrates and elevated expression despite adipogenic media. Size-restricted adhesive islands were successfully patterned onto gel surfaces using the LSL method (Fig 3). Eosin Y autofluorescence in the DAPI channel outlined patterns.

Conclusions: PEGDA hydrogels were synthesized with varied stiffness over a physiologic range and exerted substrate-related effects on MSC lineage-specific differentiation. The LSL patterning method is successful at restricting cell shape and should provide a reliable platform to investigate combinatorial effects of stiffness and restricted cell shape on MSC differentiation. Furthermore, this system should be easily translated to 3-dimensional studies since cells can be easily encapsulated.

References:
1. Discher, D.E., et al. *Science*. 310: 1139-1143.
2. Engler, A.J., et al. *Cell*. 126: 677-689.
3. McBeath, R., et al. *Developmental Cell*. 6: 483-495.

CONTINUOUS MONITORING OF FIBROBLASTS SEEDED IN CHITOSAN SCAFFOLDS USING ELECTROCHEMICAL IMPEDANCE SPECTROSCOPY

Karthik Gotrala [1], and P. Sidney Sit[1, 2]
[1]Biomedical Engineering and [2]Institute for Micromanufacturing
Louisiana Tech University, Ruston, LA 71272
Email: kgo003@latech.edu[1], sidney@latech.edu[2]

Statement of Purpose: In tissue engineering, porous scaffolds are used to mimic the functions of natural tissue by providing structural support to the embedded cells [1]. Most available techniques to assess the response of cells within the scaffolds involve damage to the scaffolds that they are prevented from further use. Hence, there exists a need to develop a protocol for continuous, non-destructive monitoring of cell responses. Previously, electrochemical impedance spectroscopy (EIS), a direct non-destructive method, which involves the passage of current through porous materials, has been successfully used to characterize the pore size and the porosity of chitosan scaffolds [2]. The purpose of the present study is to use EIS to provide continuous, non-destructive monitoring of fibroblasts seeded in chitosan scaffolds.

Materials and Methods: Chitosan solution was prepared by dissolving 2%w/v chitosan powder (>85% degree of deacetylation (DD); Sigma) in 2%v/v acetic acid, which was heated at 50 ˚C. Chitosan solution was then subjected to freezing at -20^{o}C overnight, followed by lyophilization [2]. The obtained scaffolds (3 cm in diameter, 1.5 cm thickness) were waxed on sides and bottom prior to cell seeding to prevent any current leakage during EIS. NIH 3T3 fibroblasts (American Type Culture Consortium (ATCC)) were cultured under 37 ˚C and 5% CO_2 in Dulbecco's Modified Eagles Medium ((DMEM); ATCC) supplemented with 10% calf bovine serum (ATCC) and 4mM L-glutamine. After the cells became confluent, they were collected by trypsinization. All the scaffolds were sterilized using ultraviolet irradiation for 5 min, followed by incubation in 1 ml complete culture medium prior to seeding.

For EIS measurement, chitosan scaffold was first placed in polystyrene Petri dish (6 cm in diameter, 3 cm in thickness). Two 6Al 4V ELI medical grade titanium wire probes (Small parts, inc, Miramar, FL), used as left and right electrode, were pierced into the scaffold while maintaining a distance of 1 cm. The components of EIS include an AC generator and an impedance analyzer (Solartron, 1260A, Hampshire, England) that were connected to these titanium electrodes. Frequency range of 10^{-3} to 10^{6} Hz generated by the AC generator, while operating at constant current, was used to sweep through the fibroblast-seeded scaffold. Input signal was fed to the computer during data collection, which was used to calculate the complex impedance at each frequency. The data obtained from the impedance analyzer include the impedance magnitude, real and imaginary component of the impedance and the phase shift.

EIS was conducted on 3 batches of scaffolds, each of which consisted of six scaffolds that were equally divided into two groups: with and without cell seeding. Initially, three wax-coated scaffolds without cells were saturated in phosphate-buffered saline. EIS was performed with 0.1 mA constant current and frequency ranging from 10^{-3} to 10^{6} Hz. Then, fibroblasts were placed atop of the scaffold so that they can penetrate into the scaffolds over time. Fibroblast-seeded scaffolds were placed in the incubator for 8 hrs at 37 ˚C and 5% CO_2 [3]. EIS was repeated on fibroblast-seeded scaffolds using the same experimental parameters as in scaffolds without fibroblasts. EIS measurement was performed again after the fibroblast-seeded scaffolds were fixed using 4% paraformaldehyde (Sigma).

Results and Discussion: The data obtained from EIS produce a Nyquist plot of real (x-axis) vs imaginary (y-axis) impedance, which is expected to take a semi-circular curve intercepting x-axis. Previously, it was shown that for unmodified scaffold swollen with non-diluted PBS, the semi-circular curve intercepted the x-axis at 10,600 ohms, which corresponded to the bulk resistance [2]. When the scaffolds are seeded with fibroblasts, this bulk resistance and the porosity of the scaffold are expected to change. The change in porosity is simply due to the physical presence of the fibroblasts in the pores. The change in bulk resistance can be attributed to the capacitive effect of the cells. The phospholipid content of the cell membrane is a non-conductive dielectric. Since this membrane lies between intra- and extra-cellular fluids, a conductive/dielectric/conductive layer is formed, thus producing a capacitive effect [4]. Upon seeding the pores of the scaffold with fibroblasts, the passage of current through the pores is blocked, resulting in a change in bulk resistance.

Conclusions: Protocols for seeding chitosan scaffolds with fibroblasts and continuous monitoring of fibroblasts seeded onto chitosan scaffolds using EIS have been developed. Changes in impedance value indicate the presence of cells in the scaffold, which could be estimated through bulk resistivity and the porosity of the scaffold. The results suggest that EIS can be used as a non-destructive characterization method for the continuous monitoring of the native and fibroblast-seeded form of chitosan scaffolds.

References:

1. R Lanza, R Langer, J Vacanti, Ed. Principles of Tissue Engineering. 3rd ed. Academic Press (2007).
2. Tully-Dartez et al., Tissue Eng: Part C. (2009). In press.
3. Thein-Han et al., J. Biomed. Mat. Res Part B. 80: 92-101 (2007).
4. S Grimnes and OG Martinsen, Bioimpedance and Bioelectricity Basics. 2nd ed. Academic Press (2008).

POST POLYMERIZATION CROSSLINKED POLYURETHANE SHAPE-MEMORY POLYMERS

+ *· **Hearon, K; *Gall, K; **Wilson, T S; +Maitland, D J
+Texas A&M University, College Station, TX; *Advanced Materials Lab, Georgia Institute of Technology, Atlanta, GA;
**Lawrence Livermore National Laboratory, Livermore, CA
hearon.keith@tamu.edu

Objectives: The objectives of this work were the synthesis and characterization of novel polyurethane (PU) shape-memory polymers (SMPs) that could be made into thermoplastic polymers, processed into complex thermoplastic precursors, and later crosslinked in a final curing step using either heat or electron beam irradiation..

Methods: Difficulties in SMP processing have occurred because chemically crosslinked SMPs are currently produced in a one-step polymerization of monomers and crosslinking agents. Chemically crosslinked SMPs offer numerous advantages over physically crosslinked SMPs, which include superior cyclic recoverable strains, higher rubbery modulus values, and higher toughness values. To address the processing limitations of chemically crosslinked SMPs, an extensive search for commercially available monomers with predicted potential for post-polymerization crosslinking was conducted, and thermoplastic polyurethanes were synthesized from these monomers. These thermoplastic PU's were then exposed to heat at 200 ºC or electron beam irradiation at 50 kGy in an attempt to induce chemical crosslinking.

The resulting network polymers were characterized through DMA, DSC, uniaxial tensile tests, sol-gel analysis, and FT-IR to determine if crosslinking occurred and to evaluate thermo-mechanical properties. The specific crosslinking mechanism of this new class of SMPs is being characterized by examining the effects of chemical composition, absorbed radiation dosage, irradiation temperature, and thermal crosslinking temperature on crosslink density. Crosslink density will be quantitatively measured using solid-state NMR. Once fundamental links tying chemical structure to thermo-mechanical properties are established, custom monomers with specific chemistries will be synthesized to further optimize properties for specific applications.

Results: DMA results and sol/gel analysis of polyurethanes synthesized from 2-butene-1,4-diol, trimethylhexamethylene diisocyanate, and dicylcohexylmethane diisocyanate have provided concrete evidence that chemical crosslinking occurred in select irradiated samples and in all heated samples. Further thermo-mechanical characterizations demonstrated outstanding properties, including tailorable glass transitions between 25 and 80°C, tailorable rubbery moduli between 0.2 and 4.2 Mpa, recoverable strains of up to 93%, failure strains of over 500% at Tg, and qualitative shape-recovery times of less than 12 seconds at body temperature.

Conclusions: This new polyurethane SMP class is the first in what appears to be a very industrially relevant class of highly processable shape-memory materials. These new polyurethanes can be injection molded into complex thermoplastic precursors and later crosslinked either by heat or electron beam irradiation. These new materials were determined to have outstanding mechanical properties and appear to be very well-suited for biomedical applications.

THE VERSATILITY OF TWO-PHOTON ABSORPTION LASER SCANNING LITHOGRAPHY)

Joseph C. Hoffmann[1] and Jennifer L. West[1]
[1]Department of Bioengineering, Rice University, Houston, Texas, USA.

Objective: A variety of photolithographic technologies have been applied to biomaterials in order to pattern bioactive ligands into spatially controlled topographies. Two-photon absorption laser scanning lithography (TPA-LSL) allows for the creation of three dimensional microenvironments through the use of a computer controlled, tightly focused laser beam to initiate crosslinking of ligands in a minute focal volume. In this work, TPA-LSL is applied to the micropatterning of fluorescently labeled monoacrylate PEG-RGDS in poly (ethylene glycol) diacrylate (PEG-DA) hydrogels. Specifically, we characterize the effect of laser scan speed and power on fluorescence intensity, and therein, PEG-RGDS concentration. We also demonstrate the versatility of TPA-LSL by producing micropatterns of varying size and 3D shape. Finally, we report the micropatterning of multiple, overlapping moieties with differing fluorescent labels to serve as a proof of concept for patterning an array of bioactive ligands within a PEG-DA hydrogel.

Methods: *PEG-DA Hydrogel fabrication:* A glass coverslip was piranha etched and incubated with 85 mM 3-(Trimethoxysilyl)propyl methacrylate (ph 4.5) in ethanol to introduce surface acrylate groups to the glass. A prepolymer solution of 10% (w/v) PEGDA in HBS with 10 µL mL^{-1} of 300 mg mL^{-1} 2, 2-dimethoxy-2-phenylacetophenone (DMAP) in *N*-vinyl pyrrolidone (NVP) was then prepared and injected between an acrylated coverslip and a glass slide separated by a .5 mm spacer. The hydrogels were pre-crosslinked and immobilized to the acrylated coverslip through a 45 second exposure to UV light (365 nm). *Fluorescent monoacrylate PEG-RGDS synthesis:* Acrylate-PEG-SCM (Laysan) was reacted with RGDS at a ratio of 1.2:1 in DMSO. The resulting monoacrylate PEG-RGDS was then further reacted with one of several amine reactive fluorophores in 0.1 M sodium bicarbonate buffer (ph 8.3) and purified via dialysis. *TPA-LSL Patterning Strategy:* The pre-crosslinked hydrogel was incubated in a solution of fluorescent monoacrylate PEG-RGDS (5-10 nmol/mL) in HBS with 10 µL mL^{-1} of 300 mg mL^{-1} DMAP in NVP. The hydrogel was then positioned on the stage of an LSM 510 META NLO confocal microscope. Patterns were designed using the region of interest function in the LSM software, and the laser power, scan speed, microscope objective and Z plane were specified to create patterns of desired dimensionality and concentration. A two-photon titanium/sapphire laser tuned to 720 nm was then scanned across regions of interest to initiate crosslinking of free acrylate groups in desired, free-form 3D patterns. The hydrogel was then washed with HBS to remove unbound fluorescent acrylate-PEG-RGDS and the resulting pattern was imaged using a confocal microscope. *Patterning of Multiple Fluorescent Ligands:* Patterned hydrogels were then incubated in a similar solution of monoacrylate PEG-RGDS (5-10 nmol/ml) labeled with a fluorophore of a different excitation and emission spectrum. As described above, the two photon laser tuned to 720 nm was then be used to create a second pattern with dimensionality and degree of crosslinking specified via patterning conditions.

Results: *TPA-LSL patterns of varying size*

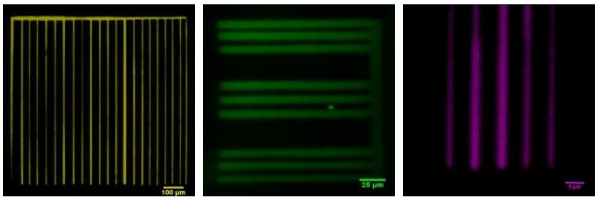

Figure 1. Patterns of fluorescent acrylate-PEG-RGDS in PEG-DA hydrogels created via TPA-LSL with 10X (L), 20X(C) and 63X(R) objectives. Scale bars 100 µm (L), 25 µm(C) and 5 µm(R).

Patterns of Varying PEG-RGDS Concentration

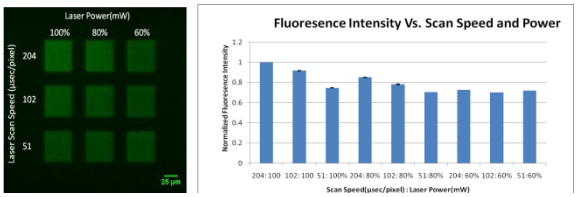

Figure 2. Patterns vary in PEG-RGDS fluorescence intensity and therefore concentration due to changing pattering conditions.

Three Dimensionality of TPA-LSL

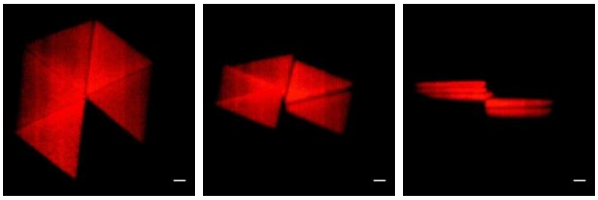

Figure 3. 3D projection of fluorescent-acrylate-PEG-RGDS pattern in PEG-DA.

Patterning of Multiple Fluorescent Ligands

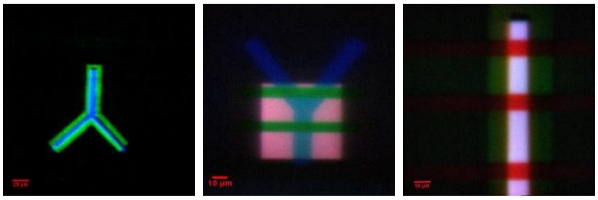

Figure 4. Patterns of two juxtaposed fluorescently labeled acrylate-PEG-RGDS ligands (left) and three different overlapping ligands (center and right) in PEG-DA hydrogels.

Conclusions: In this work, we significantly advance the versatility of TPA-LSL. Specifically, we demonstrate the ability to pattern fluorescent acrylate-PEG-RGDS ligands with distinct three dimensional shape in size ranges between 1 mm and 2 µm. Additionally, we show the ability to control concentration based on scan speed and laser power. Finally, we show the ability to pattern multiple overlapping fluorescent ligands with micrometer range precision within a single PEG-DA hydrogel. Future research will explore the application of newfound TPA-LSL patterning techniques in degradable PEG based hydrogels with a variety of different cell types. Specifically, we plan to evaluate cell phenotype and migration when exposed to multiple types of bioactive ligands in three dimensions.

FRICTIONAL LOAD EVALUATION OF SHAPE MEOMRY POLYMER DEIVECS DELIVERDED VIA CATHETER

Hwang, W; Maitland D J
Texas A&M University, College Station, TX
wonjun@tamu.edu

Objective: The objective of this work is to evaluate frictional loads of shape memory polymer (SMP) foam devices delivered via catheter. The ultimate goal is to determine if it is possible to deliver compressed foams through catheters without adjunct mechanical devices

Methods: Measuring frictional load between SMP foam and catheter will show whether SMP device can be delivered to aneurysm site in vivo. The pathway of catheter is simplified as straight line in this experiment.

SMP foam devices were fabricated to take on the shape of cylinder and spherical shapes, and were subsequently glued and crimped on to the end of a guide wire. The devices were inserted in to a tube (inner diameter 6 mm), and allowed to expand at 70°C (T_g = 55°C) in order to test expansion under within the catheter above T_g. The final devices were placed inside of a 37°C bath attached to a MTS Synergie 400 tensile tester to observe the fictional load between the devices and the tube. The tensile tester is equipped with a 2N load cell, and was used acquire measured data of the system for displacements of the devices for 10 cm within the tube.

Results: It was shown that the cylindrical shaped devices have exponentially increasing frictional loads over the span of the experiment. The cylindrical devices have more contact with the tube throughout the experiment and were compressed axially when pulled through the tube. The spherical shaped devices had 10 times less frictional load as the cylindrical shaped devices, and did not suffer the same compression.

Conclusions: Frictional forces between the SMP devices and the catheter that will deliver it to the site of aneurysm treatment are an important aspect in the design of a successful therapeutic device. Geometry of the device has proven to be a critical component of frictional characteristics. Future device design will aim to minimize the frictional load between the device and the catheter.

HEALING OF MOUSE SKULL DEFECTS WITH ENGINEERED CARTILAGE

*****Kelley, C; *Gomez, H; **Johnson, E; **Cody, D; *Duke P J
[*]University of Texas – Houston Dental Branch, Houston, TX
[**]University of Texas M.D.Anderson Cancer Center, Houston, TX
Connor.F.Kelley@uth.tmc.edu

The use of cartilage to heal bone provides a different approach to current bone replacement therapy and presents certain advantages as well. These advantages include the ability to be implanted without a scaffold, to grow large pieces, and to vascularize and integrate easily.

Objective: The purpose of this study was to determine the ability of cartilage nodules differentiated from embryonic limb bud cells to heal a mouse skull defect.

Methods: Aggregates of C57BL/6HL mouse limb bud cells from E12-E12.5 embryos were cultured in the rotating bioreactor for 3 weeks, then implanted into a 2 mm skull defect in 6 syngeneic mice (6 controls had no implants). Mice were scanned with micro-CT weekly for 6 weeks. One mouse from each group was sacrificed at 2, 4, and 6 weeks, the defect region removed, decalcified and prepared for histology.

Results: Micro-CT scans showed increasing mineralization of implanted nodules with the defect being completely filled by 6 weeks. Defects in control mice were not healed at six weeks. In histological sections of 2 week control skulls, only a thin layer of cortical bone over the defect was seen; in 2 week skulls with implants, a mass of tissue, including some cartilage, filled the defect. Much of the cartilage had been already replaced by bone, and the implant was well integrated with the adjacent cortical bone.

Conclusions: Confirming the ability of cartilage to heal bone defects establishes a foundation for future applications of the use of cartilage derived from bone marrow stem cells for bone replacement in humans.

Supported by: The University of Texas Biotechnology Office (JD), NIH T32DE015355 (CK), and Cancer Center Support Grant 16672 (DC).

PHOTONIC SHELL-CROSSLINKED NANOSTRUCTURES FOR OPTICAL IMAGING AND MONITORING

[§]Lee, N S; [¥]Sun, G; [§]Lin, Y; [‡]Neumann, W L; [†]Freskos, J N; [†]Shieh, J J; [†]Dorshow, R B; [§*]Wooley, K L
[†]Covidien Imaging Solutions R&D
[‡]Southern Illinois University Edwardsville, Department of Pharmaceutical Sciences, School of Pharmacy
[¥]Washington University in Saint Louis, Department of Chemistry
[§]Texas A&M University, Departments of Chemistry and Chemical Engineering
[*]wooley@chem.tamu.edu

Optical imaging is a robust method to illuminate important biological processes at the molecular level. We have synthesized unique pH-responsive photonic shell-crosslinked nanoparticles, wherein fluorescent pyrazine dyes were used as the crosslinking chromophores to guarantee the structural integrity of the micelles and also as a fluorogenic reporting group, whose fluorescence emission depended on the local environment governed by the solution pH. This presentation will highlight the pH-responsive photophysical responses of the nanoparticles, while utilizing a pyrazine-based photo-active crosslinking unit that also brings positively-charged character to the nanostructures. Furthermore, poly(ethylene oxide) is incorporated into the corona, and the effect of oligo-arginine pyrazine dyes on the overall surface charge is investigated. With the current interest in synthetic cationic transfection agents for gene therapy, we believe that the marriage of the oligo-arginine pyrazine dyes and the pH-responsive micelles will lead to a powerful optical imaging and monitoring agents *in vivo*.

INVESTIGATION OF THE EFFECTS OF PARTICLE DIMENSIONS ON THE LOADING AND RELEASE OF THERAPEUTIC AGENTS

Lin, Y L; Lee, N S; and Wooley, K L
Department of Chemistry and Chemical Engineering,
Texas A&M University, College Station, TX 77842-3012
wooley@mail.chem.tamu.edu

Objective: Doxorubicin (DOX) is one of the most commonly used chemotherapeutic drugs, and has demonstrated a high degree of anti-tumor activity against various forms of cancer. Unfortunately, the cardiotoxicity of the drug limits its direct administration and cumulative dosage. To reduce the toxicity of DOX to normal tissue while improving its therapeutic efficacy, DOX has been incorporated into nanoparticles. These nanoparticles were prepared *via* self assembly of amphiphilic block copolymers into polymeric micelles in aqueous solution, which, after crosslinking, serve as nanocarriers for the delivery of therapeutics. In this study, we have investigated the effects of shell crosslinked knedel-like nanoparticle (SCK) dimensions on the loading and release profiles of DOX. By tuning the size of the hydrophobic core domain and hydrophilic shell domain and the crosslinking density, it is hypothesized that the rate of release and the extent of release of DOX will be affected and that optimized packaging and release properties can be achieved.

Methods and Results: Four poly(*t*-butyl acrylate-*b*-styrene) diblock copolymers were synthesized *via* reversible addition-fragmentation chain transfer (RAFT) polymerization. P*t*BA macro-chain transfer agents (CTAs) were first prepared and then chain extended with styrene. Removal of the *t*-butyl groups of the P*t*BA-*b*-PS resulted in the production of amphiphilic PAA-*b*-PS block copolymers. DOX was encapsulated into the SCKs and these drug–nanoparticle solutions were washed extensively with PBS buffer in a centrifugal filter device at 37 °C. The loading capacities of the SCKs were investigated by UV-Vis spectroscopy, and it was determined that SCKs with larger cores resulted in higher DOX loading capacities. The release of the encapsulated DOX from the SCK nanoparticles was assessed by monitoring the decrease over time of the concentration of DOX in dialysis cassettes.

Conclusion: A series of PAA-*b*-PS block copolymers was prepared *via* RAFT polymerization methods. Different hydrophobic and hydrophilic block lengths led to the production of different sized SCKs upon self assembly and crosslinking. These nanoparticles were analyzed by numerous techniques. It was determined that the differences in the size of these nanoparticles have a significant impact on the loading capacities and release rates, as well as of the extents of release of doxorubicin, which allows better control on the administration of therapeutic agents.

FROM MEMS TO BIOMECHANICS: PROBING THE LATERAL PRESSURE OF SUPPORTED LIPID BILAYERS USING MICROCANTILEVERS

Kai-Wei Liu and Sibani Lisa Biswal
Rice University, Houston, TX
kl3@rice.edu and slb@rice.edu

Objective: Supported lipid bilayers (SLBs) are popular model membranes to study lipid assemblies, as well as membrane-active peptides and proteins. Recently there has been interest in understanding how the internal lateral pressure of a lipid membrane affects membrane protein functionalities. We present a novel method to probe the lateral pressure of a SLB using a microfabricated cantilever device. A model that relates the measured nanomechanical responses to the membranes physical parameters is also a primary objective.

Methods: We use free standing microcantilever beams, which have been used as an ultrasensitive method for measuring the stresses of thin films, to measure the equivalence lateral pressure of supported phospholipid bilayers. The cantilever is silicon based, with dimension 500×100×1mm, and coated with a thin gold layer. To prevent vesicle adsorption to the gold surface of the cantilever, dithiolaromatic-PEG molecules are tethered to the gold. As the lipid membrane physisorbs to the silicon dioxide surface of the cantilever beam, a lateral in-plane stress occurs in the surface lattices of the substrate, leading to a compressive deflection. The deflection of a cantilever tip is tracked by a reflected laser beam, which is then captured with a position-sensitive detector. We relate the measured deflection, Δz, to the membrane lateral pressure, π_m:

$$\pi_m = \frac{Et^2}{3(1-\nu)L^2}\Delta z$$

This model is tested with different lipid intermolecular forces, such as electrostatic repulsion and hydrophobic interactions between lipid chains. To perform this measurement, firstly we tune the lateral pressure of a SLB by mixing zwitterionic, cationic and anionic lipids into the membrane, to evaluate the electrostatic partitioning of the lateral pressure. Secondly we investigate how cholesterol interferes with the lipid-lipid hydrophobic interaction and hydrocarbon-water exposure, for which all result in shift in lateral pressure of SLBs.

Results: A POPC membrane supported on the silicon dioxide surface results in an equivalence lateral pressure of 17.08 ± 1.39 mN/m (Figure 1, a.) Introducing cationic DOTAP lipids changes the electrostatic partitioning of membrane resulting in a larger lateral pressure, as measured using microcantilevers in Figure 2. As shown in Figure 3, there is a decrease in the lateral pressure from 17.08±1.39 mN/m to 9.91±1.33 mN/m as cholesterol content in the membrane is increased from 0 to 50%, indicating the cholesterol contracts the SLB, resulting in a tensile stress on the cantilever.

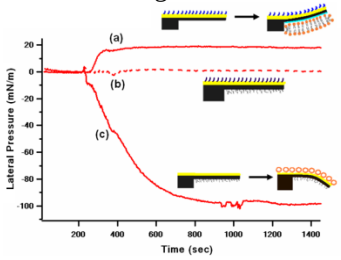

Fig. 1

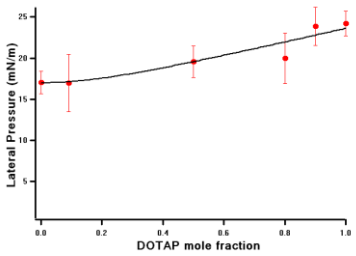

Fig. 2

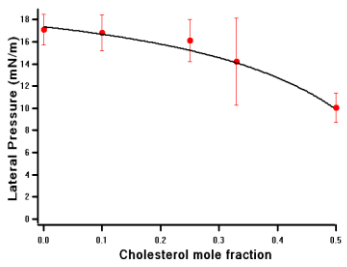

Fig. 3

Conclusions: The use of microcantilevers as a sensitive biosensor to probe lateral force interactions in lipid membranes has been investigated. We transform the detectable deformation of this MEMs device into physical properties of a membrane. Our findings yield a novel method of characterizing the lateral pressure of planar lipid membrane and shed light on how the electrostatic and structural interactions in the membrane change its lateral force interactions.

STRONG NEAR-IR ABSORBING BIO-COMPATIBLE GOLD NANOPARTICLES

Sreekar Marpu[1], Rob Petros[2*], Mohammad A. Omary[2*] and Zhibing Hu [3*]
Departments of Material Science and Engineering[1], Chemistry[2], and Physics[3]
University of North Texas, Denton, Texas 76203
sreekarmarpu@gmail.com

Objective: Strong Near IR absorbing gold nanoparticles stabilized in biocompatible medium are promising novel nanomaterials for many diagnostic and therapeutic applications. Gold nanorods popularly stabilized in presence of CTAB, a cationic surfactant suffer from serious cytotoxicity to cells even at very low concentrations. Replacing CTAB completely would result in destabilization and agglomeration. So there is a high technological advance in directly stabilizing these Near-IR absorbing gold nanoparticles in biocompatible medium inorder to minimize toxicity and be able to translate these novel nanomaterials to clinical studies. In a single step photochemical route, strong Near-IR absorbing gold nanoparticles are synthesized and stabilized in a highly bio-compatible chitosan polymer and inside a thermo-responsive stimuli sensitive PNIPAM microgel separately starting from Au(I) based thiolate precursor.

Methods: Gold nanoparticles having strong absorptions between 700-900 nm are easily synthesized by photochemical decomposition of $Au(Me_2S)Cl$ both in chitosan and PNIPAM-co-allylamine microgel separately on exposure to high pressure Hg lamp, The reactions are performed without aid of any other reducing agents or other toxic chemicals in a single step. Different wavelength absorption gold nanoparticles are obtained based on concentration and pH of the reaction mixture.
Both visible and strong Near-IR absorption gold nanoparticles are synthesized from same starting mixture just by varying pH, concentration or conditions of exposure to light.
Shape, size and distribution of these nanoparticles are characterized by Uv-VIS, DLS, FSEM and HRTEM. MTT assay has been performed using proximal tubule cells (LLC -PK1) cell lines comparing with both CTAB stabilized and PEG-amine stabilized gold nanorods obtained from Nanopartz.

Results: Tuning of Near-IR absorption in both PNIPAM and Chitosan are shown in the figure (A) , and the TEM images obtained from the same are shown in figure (B)

Figure-A

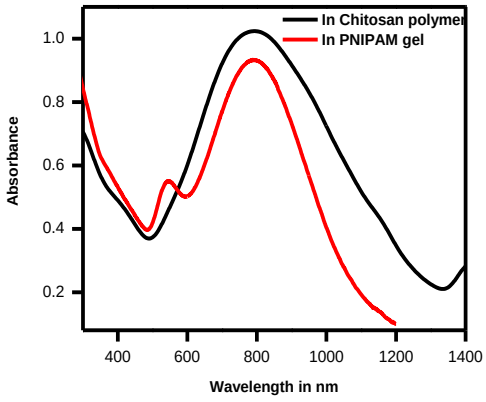

Figure-B

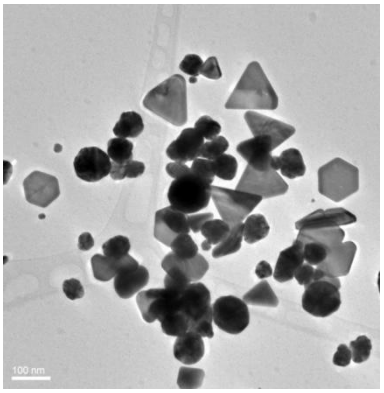

MTT assay performed to test cytotoxicity of chitosan stabilized gold nanoparticles showed much better cell viability and cell proliferation results compared to gold nanorods obtained from Nanopartz.

Conclusions: Bio-compatible gold nanorods obtained here are shown to be promising agents for photothermal therapy and many other diagnostic and therapeutic applications based on their cell viability and photothermal release tests.

PATTERNED ADENO-ASSOCIATED VIRUS FOR CONTROLLED GENE DELIVERY

+McConnell, KI; +Slater, JH; *Han, A; +West, JL; +Suh, J
+Rice University, Houston, TX
*Texas A&M University, College Station, TX
kim1@rice.edu

Objective. Spatial organization of gene expression is a crucial element in the development of complex native tissues. As tissue engineering strategies continue to expand and overcome significant barriers, the capacity to achieve spatially controlled gene expression profiles in a tissue engineering construct is still a considerable difficulty. To address this critical need, we are developing a platform technology based on the adeno-associated virus (AAV) that will enable tissue engineers to obtain specific, spatially organized expression of genes in a population of cells. This flexible platform allows for the specific patterning of various gene and shRNA cassettes, resulting in spatially defined gene expression profiles that may promote the generation of highly functional tissue.

Methods. We used polydimethylsiloxane (PDMS) stamps to pattern various alkanethiol solutions onto gold-coated substrates. The spatial dimensions of these patterns can be tailored easily to the desired tissue engineering application. For this work we used stamps with 600 micron diameter circle features. Viral particles carrying genes of interest were immobilized on the patterned substrates, creating a spatially organized arrangement of gene delivery vectors. We attached both human fibronectin (HFN) and AAV2-GFP (encoding GFP) to alkanethiol patterned substrates. A variety of surface chemistries were tested, including $–CH_3$, -COOH, $-NH_2$, and –OH terminated alkanethiols in order to determine the optimal substrate. Patterns were backfilled with an –OEG terminated alkanethiol in order to prevent background protein attachment. To analyze and compare surface attachment, we used immunostaining to image immobilization of both HFN and AAV2. Images were qualitatively compared for surface coverage and ImageJ was used to generate quantitative integrated density measurements. Additionally, HeLa cells were subsequently seeded on top of the HFN and AAV2 patterns to determine the efficiency of cell attachment and gene expression using this platform.

Results. Immunostaining showed variable protein attachment resulting from different surface chemistries. For each case, protein was isolated to the patterned circles, indicating that the –OEG backfill was effective in preventing non-specific adsorption. As expected, $-CH_3$ surfaces yielded the highest levels of HFN and/or AAV2 attachment. However, when seeded with HeLa cells, transduction levels at 72 hours were statistically similar among $–CH_3$, -COOH, and $–NH_2$ surfaces. The –OH surface yielded less cell attachment and less overall gene expression.

Conclusions. Our flexible platform allows for the patterning of both cell adhesive protein and a gene delivery vector. Patterns generated were tight and gene delivery was efficient. This platform can be extended to a variety of adhesive proteins and cell types.

Electrospun Mesh-Hydrogel Composites for Ligament Tissue Engineering

Rebecca McMahon[a], Scott Guelcher[b], Aaron Goldstein[c], Mariah Hahn[a]
[a] Department of Chemical Engineering, Texas A&M University
[b] Department of Department of Chemical & Biomolecular Engineering, Vanderbilt University
[c] Department of Chemical Engineering, Virginia Polytechnic Institute and State University

Electrospinning is a polymer processing technology that is capable of producing micron-scale fused-fiber mesh biomaterials, which possess excellent tensile properties and are suitable for the regeneration of oriented tissues such as ligaments. A major drawback, which limits the broader clinical applicability of this process, is the fact that generating electrospun scaffolds with thicknesses greater than 1 mm is extremely time intensive. Creating a hybrid scaffold by layering the electrospun structures and securing them together using a hydrogel can potentially result in a scaffold with implantable mechanical properties, yet with dimensions suitable for replacing human ligaments. In general, hydrogels initially have mechanical properties below native ligament, and therefore would not be suitable for implantation without support, yet they have the ability to direct differentiation of mesenchymal stem cells. One of the benefits of the proposed techniques is the ability to optimize the properties of the layers independently to influence cell behavior while ensuring the mechanical properties are suitable for implantation. We designed an experiment as a proof of concept of this method for an implantable ligament graft. 10T½ mouse mesenchymal cells were chosen for their ability to differentiate into ligament fibroblasts, and a polyurethane-based electrospun mesh provided support to a fibrin hydrogel to create a ligament-like structure. We demonstrate the ability of these composite scaffolds to be fabricated with moduli and tensile strengths similar to that of native ligament. In addition, we show that the resulting constructs support ECM accumulation and maintain their mechanical integrity following prolonged cyclic distension. This approach has potential application to the regeneration of a range of oriented tissues, such as blood vessels.

POLY(ESTER URETHANE UREA) POLYHIPES AS HIGH POROSITY BONE GRAFTS

Robert Moglia, Nick Sears, Hugh Benhardt, Elizabeth Cosgriff-Hernandez*
*Biomedical Engineering, Texas A&M University, College Station, Texas 77843
rmoglia@neo.tamu.com

Objective: Engineered bone grafts have the potential to repair critical size defects when traditional transplants are unavailable or fail. It is widely recognized that scaffold architecture can profoundly influence the success of these constructs. Scaffold architecture (porosity, pore size, interconnectivity) and the scaffold properties that result from that architecture (e.g. biodegradation rate, mechanical properties) are dictated by the fabrication process. Emulsion templating is a relatively new method for the production of highly porous scaffolds and involves the template polymerization of high internal phase emulsions (HIPEs). HIPEs are characterized by a droplet phase volume fraction of at least 74%. The continuous phase contains a monomer that is polymerized and locks in the emulsion geometry at the gel point. The droplet phase is then removed, and the resulting porous scaffold is known as a polyHIPE. The control of scaffold architecture afforded by emulsion templating makes polyHIPE materials attractive candidates for tissue engineering scaffolds. Traditional polyHIPEs have been fabricated with chain growth or radical crosslinking processes. In the present study, we utilized a step-growth polymerization mechanism that expands the range of monomers and resulting properties available to this fabrication strategy. Poly(ε-caprolactone) (PCL), a well-established biodegradable polymer, was functionalized with isocyanate end groups to create polyHIPEs with interconnected porosity that cure at body temperature..

Methods: *Synthesis:* All chemicals were purchased from Sigma-Aldrich (Milwaukee, WI, USA) and used as received. PCL-triol (300 g/mol) was endcapped with hexane diisocyanate (HDI) in dimethylformamide at 80°C using stannous octoate as a catalyst under anhydrous conditions.[1] The solution was then purified by washing with water and the solvent removed by rotary evaporation, leaving a viscous, colorless PCL-triisocyanate (PCL-TI) product.
HIPE formation: A series of polyHIPEs were fabricated using established emulsion templating protocols.[2] The organic phase consisted of HDI and PCL-TI (1:1, 2:1, 3:1, 6:1) with toluene as the diluent (50, 60, 70%). Span 80 (20 wt% of the organic phase) was used as the surfactant. These components were mixed thoroughly in a 3 neck round bottom flask with a mechanical stirrer at 300 rpm. An aqueous solution (1 wt% $CaCl_2$) was then added at a rate of 1mL/min while stirring to a ratio of 80:20. The HIPE was cured at 37°C for at least 12 hours. After cure, samples were dried for 24 hours under vacuum. Gravimetric analysis was utilized to measure porosity and scanning electron microscopy (SEM) was used to characterize architecture of cryo-fractured specimens.
Mechanical Analysis: The compressive modulus of the polyHIPEs was determined using an RSA III dynamic mechanical analyzer (TA Instruments) with a 2500-g load cell. The samples were cut into rectangular shapes with an aspect ratio of three (approximately 9 mm in width and length by 3 mm in height) and compressed at a rate of 50 μm/s. The calculations from ASTM method D1621-04a were used to determine the modulus of the porous scaffolds. Reported moduli data was an average of three to four specimens for each tested scaffold composition along with the standard deviation of each.

Results: *Synthesis:* Successful synthesis of PCL-triisocyanate was confirmed with FTIR and NMR spectroscopy. The FTIR spectrum of PCL-TI revealed a peak at 2270cm^{-1} not present in the spectrum of PCL-triol indicative of isocyanate endgroups. In addition, a broad absorption peak typical of OH stretching at 3383 cm^{-1} in the PCL-triol shifted to the NH stretching at 3332cm^{-1} as a result of urethane bond formation after functionalization.
PolyHIPE Formation: HIPEs based on HDI:PCL-TI cured at 37°C via reaction of isocyanate end groups with water which liberated carbon dioxide to form amine end groups. Subsequent reaction of these amine end groups with the remaining isocyanate end groups resulted in a poly(ester urethane urea) network which locked in the emulsion geometry. The resulting grafts were characterized by open pores on the order of 5-40 microns, and typical porosity values greater than 90%. Foam properties ranged from rigid to elastomeric in nature based on the resultant network structure. Specifically, higher HDI concentration resulted in an increase in the distance between crosslinks.
Mechanical Analysis: The compressive modulus was studied in relation to both HDI:PCL-TI ratio and catalyst concentration. The tested HIPEs showed moduli between 100 kPa and 2.0 MPa. An HDI:PCL-TI ratio of 3:1 had the largest average compressive modulus (1.159 MPa). It was also observed that as the catalyst concentration was increased past 0.05 wt%, there was a drop in average compressive modulus from 1.2 MPa to 460 kPa. This shows that composition of these polyHIPEs has a significant and complicated effect on their mechanical properties.

Conclusions: Emulsion templating of multifunctional polyester prepolymers was utilized to generate a new class of step-growth polyHIPEs. These high porosity scaffolds are of particular interest in bone tissue engineering due to the rigidity of the resulting foams, ease of fabrication, and control over architecture. Current studies are focused on improving scaffold properties incorporating a second polymer network to replace toluene.

The authors acknowledge the financial support of the National Science Foundation (BRIGE 0926824).
References: [1] Skarja et al. *Journal of Biomaterials Science, Polymer Edition*, **9**(3), 271-295 (1998).
[2] Christenson et al. *Biomacromolecules*, **8**(12), 3806-3814 (2007).

PERMEABILITY EVALUATION OF SHAPE MEMORY POLYMER POLYURETHANE FOAMS

Muschenborn, A D; Johnson, J A; Maitland, D J
Texas A&M University, College Station, TX
amuschenborn@tamu.edu

Objective: To quantitatively evaluate the hydraulic permeability of temperature activated Shape Memory Polymer (SMP) Polyurethane (PU) foams using Darcy's Law.

Methods: Pressure differentials will be measured across cylindrical samples of SMP foam while subject to deionised water steady flow using a gravity feed system. Permeability will be calculated from Darcy's law:

$$\kappa = \frac{Q\eta L}{\Delta P A}$$

where κ is the hydraulic permeability, Q is the flow rate of the fluid going through the sample, η is the viscosity of the fluid, *L* is the length between the points where pressure readings will be taken, *A* is the sample's cross-sectional area and ΔP is the pressure difference.

Results: The measured average permeability value was $2.5 \cdot 10^{-10} \pm 1.23 \cdot 10^{-10} m^2$.

Conclusion: Although characterization of the structure of SMP PU foams must be done by considering numerous factors such as density, pore size, porosity and tortuosity, permeability measurements provide an insight into their functionality, given that permeability is strongly affected by porosity, pore size and interconnectivity.

THE EFFECT OF SUBSTRATE STIFFNESS ON CARDIOMYOCYTE ACTION POTENTIAL

*Myers, J; *+Jacot, J
* Rice University, Houston, TX
+ Texas Children's Hospital, Houston, TX
jeff.jacot@rice.edu

Objective: Cardiomyocytes have been shown to generate maximum contractile force when the stiffness of the substrate on which they are cultured matches that of native cardiac tissue, partially due to a combination of sarcomere length and calcium storage effects1. We hypothesized that substrate stiffness also affects ionic currents during cardiomyocyte action potentials. We tested this hypothesis by patch clamping cardiomyocytes grown on substrates of varying stiffness and recording individual action potential voltages.

Methods: Neonatal rat ventricular cardiomyocytes were cultured on polyacrylamide gels with varying concentrations of acrylamide monomer and bisacrylamide crosslinker, resulting in elastic moduli of 1, 5, 10, 25 and 50 kPa. Average beating rates, cell areas, and cell circularities were recorded at various time points on each gel. Action potentials of individual cardiomyocytes on each gel were recorded using whole cell patch clamping in current clamp mode at one week after plating.

Results: No significant difference was observed in the beating rates of neonatal rat cardiomyocytes on gels of varying stiffness of 1 to 50 kPa between 2 and 14 days in culture. However, the decay time of the action potential was significantly lower in cardiomyocytes cultured on gels of 10kPa, approximately the elastic modulus of native cardiac tissue, compared to gels of 1 kPa and 50 kPa (Fig 1). This decay time is inversely correlated with contractile force, calcium transient magnitude and internal calcium stores reported in previous studies.

Conclusions: The repolarization of neonatal rat cardiomyocytes, as measured by the action potential decay time, is significantly faster when the cardiomyocytes are cultured on gels with stiffness approximating the native myocardium, compared to both softer and stiffer gels. Because cardiomyocyte repolarization time is regulated by inward calcium flux, and because the decay time inversely correlates with stored calcium, these differences are likely due to differences in calcium flux across the membrane. Future experiments will focus on calcium flux, as well as the relative expressions of calcium and potassium channels in these cells.

Reference:

1 J. Jacot, Substrate Stiffness Affects the Functional Maturation of Neonatal Rat Ventricular Myocytes Biophysical Journal, 2008

SYNTHESIS AND FOLDING CHARACTERISTICS OF POLYDEPSIPEPTIDES

M. Nguyen, M. Abdelmelek, K. Masada, D. Campbell, P. Ren, L. Suggs
University of Texas at Austin, Austin, TX.
marymnguyen@yahoo.com

Objective: Polydepsipeptides (PDPs) have alternating ester and peptide bonds and have previously been shown to maintain regular secondary folding[1]. This study aims to synthesize and investigate the secondary folding characteristics of polydepsi(Gly), polydepsi(Lys), and polydepsi(Asp) showing that regular secondary structure can be modeled and maintained within PDPs.

Methods: Reagents. Bromopropionyl-glycine (BPG), and poly-L-alanine (poly(Ala)) were purchased from Sigma Aldrich (St. Louis, MO). Fmoc-L-Lys(Z)-OH, Fmoc-L-Asp(OBzl)-OH, and dimethylaminopyridine (DMAP) were from Novabiochem/EMD Biosciences (San Diego, CA). Trityl chloride resin and diisopropylcarbodiimide (DIC) were from Anaspec (San Jose, CA).

Polydepsi(Gly). The cyclic intermediate was prepared with BPG dissolved in excess DMF to a slurry of potassium carbonate and DMF under nitrogen at 65ºC for 24 hours. Potassium carbonate was removed by centrifugation. The cyclic intermediate was concentrated and polymerized with $SnOct_2$ in a siliconized vessel at 120ºC for 24 hours under vacuum.

Polydepsi(Lys) and polydepsi(Asp). The polymers were synthesized using solid phase chemistry on a trityl chloride resin. The resin was functionalized with L-lactic acid using DIPEA in DCM and coupled to the desired Fmoc-peptide with DMAP and DIC. The N- and C-terminal groups were exposed with 20% piperidine in DFM or 1% TFA in DCM, respectively. The deprotected groups were then coupled with DIC to achieve a depsipeptide repeat (Figure 1). The deprotection and coupling method are repeated until 12 depsipeptide units are achieved.

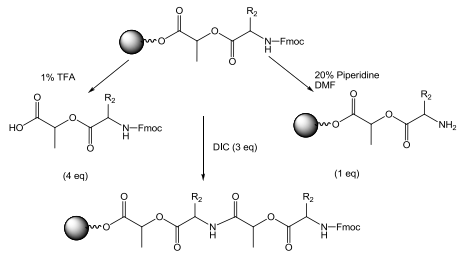

Figure 1. Stepwise growth of polydepsipeptides. R_2 = Lys(Z) or Asp(OBzl).

Circular Dichroism.Polydepsi(Gly) and poly-L-(Ala) were dissolved in water and dichloroacetic acid and concentrated in 90% trifluoroethanol.

Results/Discussion: The synthesis of cyclodepsi(Gly) and its corresponding PDP are confirmed with H-NMR and are consistent with the literature[2]. Intermediates of polydepsi(Lys) and polydepsi(Asp), specifically of 2 and 4 repeats have been confirmed with mass spectroscopy. Polydepsi(Gly) in 90% TFE reveals a β-sheet structure with a slight transition to a β-turn conformation, evident at 209 nm (Figure 2).

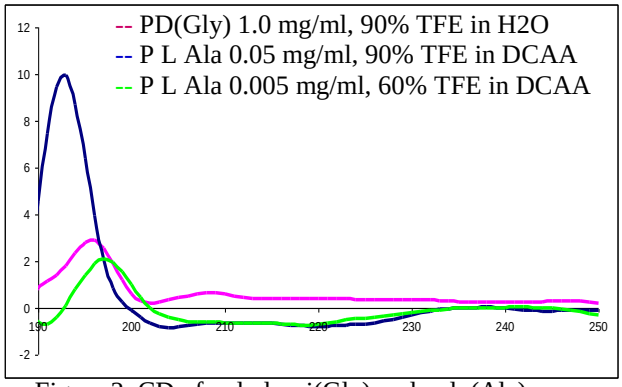

Figure 2. CD of polydepsi(Gly) and poly(Ala)

Conclusion: A major motivation towards this current synthesis of PDPs lies in the relative ease in tailoring functionality within the chemical structure. Despite substitutions of the amide bond at alternating positions by ester functionality, polydepsi(Gly) folds into naturally occurring secondary structures that are sensitive to specific environmental conditions.

References:

1. Becktel, et al., *Macromolecules* 1981, 14, (1), 203-207.
2. Barrera, et a;, . A.; *Macromolecules* 1995, 28, (2), 425-432.

AMNIOTIC FLUID-DERIVED STEM CELL VIABILITY ON POLY(ETHYLENE GLYCOL) HYDROGELS

*Petsche, J J; *Aliru, M L; +*Jacot, J G
* Rice University, Houston, TX
+Texas Children's Hospital, Houston, TX
Jennifer.Petsche@rice.edu

Objective: Amniotic fluid-derived stem cells (AFSC) are a promising new cell source for tissue engineering, expressing pluripotency markers characteristic of embryonic stem cells with the non-tumor forming properties of adult stem cells. Poly(ethylene glycol) (PEG) hydrogels are biocompatible and readily modified to present a variety of extracellular matrix and growth factor signals. The rigidity of PEG-based hydrogels can be controlled by varying prepolymer concentrations, and studies have shown a dependence on substrate rigidity for stem cell differentiation. The objective of this study was to quantify the control of the elastic modulus of a PEG-based polymer with varying prepolymer concentrations and to evaluate the viability of AFSC on these hydrogels.

Methods: AFSC were isolated from human amniotic fluid obtained from second trimester subjects undergoing removal of amniotic fluid as part of therapeutic intervention. Cells were expanded up to the fifth passage. PEG hydrogels were fabricated with PEGylated-RGDS to allow for cell adhesion and 2.5%, 5%, 10%, and 15% (w/v) solutions of poly(ethylene glycol) diacrylate (PEGDA) prepolymer. AFSC were cultured on PEG hydrogels for 48 hours then evaluated for cell viability using a live/dead assay, proliferation using a BrdU assay, and apoptosis using a TUNEL assay.

Results: The elastic modulus directly correlated with the concentration of PEGDA (Fig. 1). After 48 hours of culture, 10% and 15% gels had significantly lower numbers of cells compared to the softer 2.5% and 5% gels. No significant differences were observed in cell viability, the percentage of proliferating cells or the percentage of apoptotic cells (Fig 2).

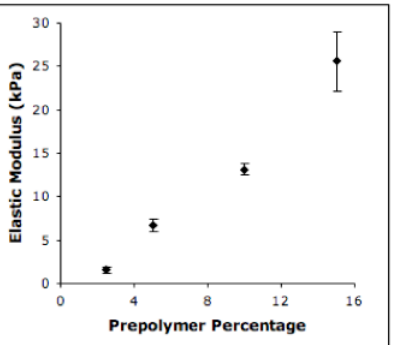

Figure 1. Graph of elastic modulus vs. prepolymer percentage in hydrogel.

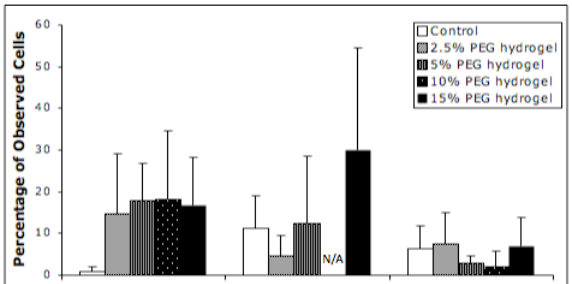

Figure 2. Graph of dead cells, proliferating cells, and apoptotic cells as percentage of observed cells of different surfaces.

Conclusions: AFSC have high attachment, remain viable and can be cultured on soft RGDbound PEG-based hydrogels made with prepolymer solutions of 2.5-5% PEGDA. However, more rigid gels made with higher PEGDA prepolymer concentrations did not support good cell attachment, though cell viability was unchanged. Further experiments will investigate cell attachment on PEG-based hydrogels with differing concentrations of RGD-bound polymer and with other attachment molecules, such as collagen, fibronectin or laminin.

MODEL DRUG RELEASE PROFILE OF PATTERNED POLYETHYLENE GYLCOL HYDROGEL

Phadungsak Phongphonkit[1] and P. Sidney Sit[1,2,3]
[1]Molecular Science and Nanotechnology, [2]Biomedical Engineering and [3]Institute for Micromanufacturing
Louisiana Tech University, Ruston, LA 71272
Email: [1]pph004@latech.edu, [2]sidney@latech.edu

Introduction: Polyethylene glycol (PEG) hydrogel has been used in many medical and pharmaceutical applications due to its high level of biocompatible and resistance to protein adsorption. Many applications of hydrogel utilize a patterned array for protein adsorption, sensing, and drug delivery. A number of techniques have been developed for patterning hydrogel such as photolithography, soft lithography, dip-pen nanolithography and ink-jet printing. Patterning using direct-write technology is a new way for micro and nanoscale fluid delivery. It can be used to print a variety of materials including proteins, DNA, RNA, viruses, chemical solutions, colloids, and particle suspension. The spot size typically ranges from 1 µm to 20 µm. In this work, fluorescein isothiocyanate (FITC) was used as a model molecule that was incorporated into polyethylene glycol-diacrylate (PEGDA) solution. It was then patterned on the surface of treated, hydrophobic glass slide. Hydrogel formation was carried out using ultraviolet (UV) irradiation. Release profile of the FITC from the patterned hydrogel was compared to that from single-spot hydrogel.

Materials and Methods: Glass surface was cleaned sequentially with organic solvents, namely, methanol, ethanol and chloroform, followed by coating with octadecyltrichlorosilane (Sigma) to make the surface hydrophobic. A macromer solution containing 13.88% (v/v) PEGDA, 6 mg/ml FITC, and 2 mg/ml Irgacure 184 was prepared. 1µl of this solution was loaded and patterned on the surface of the treated glass slide using a direct-write printing system (Nano eNabler, BioForce, Ames, IA). Experimental parameters in the patterning design consist of pattern diameter, center-to-center spacing and number of spots. Hydrogel crosslinking was obtained by placing the macromer solution under UV light for 1 minute. For single-spot hydrogel, 12 µl of the macromer solution was deposited on the surface of the treated glass slide using micropipette for UV irradiation. Release profile of FITC from these two hydrogel formats was compared. Both were placed in test plate containing 1 ml of phosphate buffered saline (PBS). PBS was collected after 1 hour and was replenished with fresh PBS. The process was repeated after 3, 5, 7, 9, and 24 hours. The concentration of FITC was then determined by fluorescent spectrometry. The percentage release of FITC is defined as the ratio of the amount released to the amount loaded.

Result and Discussion: The hydrogel solution was patterned in multiple batches, each of which was an array of 10×20 (column×row). A total of 10,000 spots were deposited. The spot size and the center-to-center distance were 12µm and 28 µm, respectively. A spot size of 5 mm was obtained for the single-spot hydrogel. Bright-field digital images of patterned and single-spot hydrogel were shown in Figure 1. The release profile of FITC from the PEG hydrogels was plotted in figure 2. In the first hour, there is a large initial burst which was approximately 67% and 47% from pattern and single-spot hydrogel, respectively. In the later phase, the release slowly leveled off. At the final time point, 76% and 66% of FITC was released from patterned hydrogel and single-spot hydrogel, respectively. Statistical analysis shows that the cumulative release of FITC is significantly larger from patterned hydrogel than from single-sport hydrogel ($p<0.05$). Since the release amount of FITC is directly proportional to the available surface area, the increase in FITC release can be attributed to the increase in the surface area of patterned hydrogel.

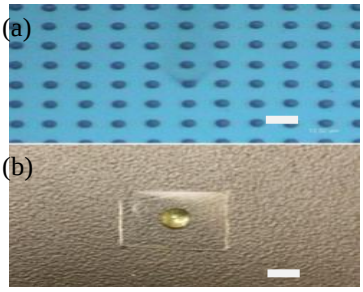

Figure 1.Digital image of (a) patterned and (b) single-spot hydrogel. Scale bar: (a) 12 µm (b) 5 mm.

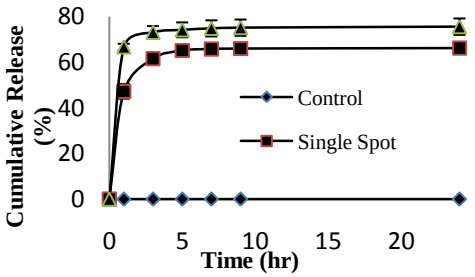

Figure 2 Comparison of cumulative release of FITC from patterned and single-spot hydrogel. Control: no loading of FITC. The release profile is significantly different between these two hydrogel formats ($p<0.05$).

Conclusion: We have demonstrated direct-write printing capability using the Nano eNabler system to create patterned hydrogel for drug release. Spot size with the range of 100 nm to 20 µm can be deposited. The amount of FITC release from the hydrogel is related to the available surface area. Patterning of hydrogel results in an increase of the surface area, which in turn leads to an increase in the cumulative release of FITC.

Reference:

1. N.A. Peppas, J Pharm Biopharm. (2000) 50: 27. 2. R. Langer and N.A. Peppas, AIChE J. (2003) 49: 2990. 3. E. Henderson, Nanomedicine. (2007) 2: 391.

THREE DIMENSIONAL RECONSTRUCTION AND CHARACTERIZATION OF SHAPE MEMORY POLYMER FOAM

+Rodriguez, J N; ++Clubb, F J; +Maitland, D J;
+Texas A&M University, College Station, TX, ++College of Veterinary Medicine, Veterinary Pathobiology, College Station, TX
jennifernrodriguez@tamu.edu

Objective: An embedding, Micro-Computed Tomography (CT) imaging, and three dimensional segmentation process has been developed for the characterization of average pore size of Shape Memory Polymer foams.

Methods: In order to remove air bubbles from the sample, an 8 mm cylindrical geometry of Shape Memory Polymer foam was crimped under 60 ºCelsius in a heated stent crimper. They retained a cylindrical shape with a diameter of approximately 1.3 mm diameter after crimping radially. These foams were allowed to expand in 5 ml of heated (44 ºCelsius) barium latex gelatin, and the volume was fixed with 5 ml of formalin. To prevent drying, the samples were wrapped in parafilm, and imaged on an X-Tek Hawk micro CT at 140 kV and 35 µA. A volume of images 1032 x 853 x 467 voxels^3 were reconstructed from the raw CT data, with a resolution resulting in 12.1µm/voxel. The 3-dimensional volumetric mesh of the foam structure was reconstructed using Amira 5.2.2 via manual segmentation. Performing a Boolean operation between the cropped 3-dimensional volumetric mesh of the foam and a solid block in Rhino 4.0 resulted in isolated 3-dimensional meshes of the individual pores. After removal of partial pores, the average pore cell size was obtained.

Results: To manage computational time, the volume of reconstructed foam was limited to a cropped version with dimensions of 300 x 273 x 389 voxels^3, having a total volume of 56.44 mm^3. The volume taken up by the reconstructed foam was 15.52 mm^3. This gives a rough porosity of 72%. Average strut thickness was 60 µm, and a standard deviation of 20 µm. Average pore cell size was 660 µm, with a standard deviation of 260 µm.

Conclusions: This work is a reasonable alternative to the current methods for measuring porosity, and average pore cell size. Further investigation will lead to an automated version of this process, and the interconnectivity of pores among these foams will be determined; both of which facilitate characterization and optimization of foam formulations.

ADHESION TO BIOACTIVE POLY(ETHYLENE GLYCOL) (PEG) HYDROGELS PROMOTES EXPANSION OFHEMATOPOIETIC PROGENITOR CELLS

Maude L. Rowland, Jean S. Altus, Jennifer L. West.
Rice University, Houston ,TX.
maude.rowland@rice.edu

Objective: Hematopoietic stem cells (HSCs) are capable of differentiating down myeloid and lymphoid lineages to become mature blood and immune cells. HSCs are used in the treatment of many blood diseases and disorders and have potential for other applications. However, HSC availability is limited due to inefficient *in vitro* culture. We propose the development of a novel, *ex vivo* culture system that recapitulates the HSC microenvironment. This niche is comprised of various cell types and biomolecules.1 By mimicking the *in vivo* environment, this culture system will facilitate self-renewal resulting in clinically relevant HSC populations.

Methods: Photopolymerized 6 kDa poly(ethylene glycol) diacrylate (PEG-DA) hydrogel wells were fabricated by replica molding the polymer against microfabricated pillars. Fibronectin-derived adhesive peptide sequences, RGDS and LDV, were covalently immobilized on well surfaces using 2.92, 1.46, 0.29, and 0.15 mM PEG-RGDS or 2.75 mM PEG-LDV solutions as previously described.2 Stromal Derived Factor 1α (SDF-1α), chemokine that regulates homing of HSCs to the niche, was covalently tethered to the PEG-DA hydrogels using the same techniques (0.33 μM solution). 7F2 cells (murine bone marrow osteoblasts) were encapsulated (1 million cells/ml) within PEG-DA or PEG-RGDS (5mM) replica molded hydrogel wells. 32D cells, a murine hematopoietic progenitor cell line, or primary murine Sca1+ cells, were seeded into the hydrogel wells at a density of 20,000 cells/cm2. Adherent cells were counted (ImageJ) as a function of culture time, biomolecule concentration, and biomolecule type.

Results: Adherent cell number increased on hydrogels modified with PEG-RGDS when compared to PEG-DA hydrogels and a fibronectin (FN) coated well plate. We also observed a dose-dependent trend of increasing cell number with increasing concentrations of PEG-RGDS (Figure 1). In samples containing higher concentrations of RGDS, cell number also increased over time indicating cell proliferation. We were also able to maintain these results when seeding primary hematopoietic cells on the gels. After 72 hours, more adherent cells were observed on gels modified with RGDS or LDV (Figure 2). A potential synergistic effect was observed on hydrogels modified with both PEG-RGDS and PEG-SDF-1α. On these scaffolds, adherent 32D cell number was increased when compared to samples modified with only one of the biomolecules (Figure 3). In coculture experiments, we observed increased 32D cell adhesion and proliferation when 7F2s were present within the hydrogel (Figure 4).

Conclusions: Within the HSC niche, adhesion to extracellular matrix proteins and stromal cells encourages HSC self-renewal and can prevent differentiation3. We have shown the ability to mimic fibronectin and stromal cell signaling by the biofunctionalization of our hydrogels with RGDS and SDF-1α and coculture with bone marrow osteoblasts. By recapitulation of the HSC microenvironment, we believe we can promote selfrenewal *ex vivo* and generate HSC populations that can be used therapeutically.

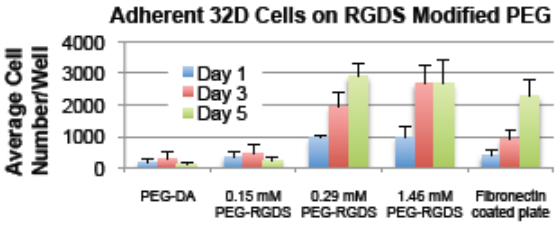

Figure 1: 32D cell adhesion and proliferation was increased on gels modified with RGDS compared to PEG-DA and fibroectin well plates

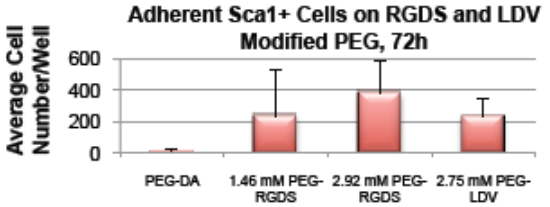

Figure 2: Sca1+ cell adhesion was increased on gels modified with RGDS and LDV compared to PEG-DA

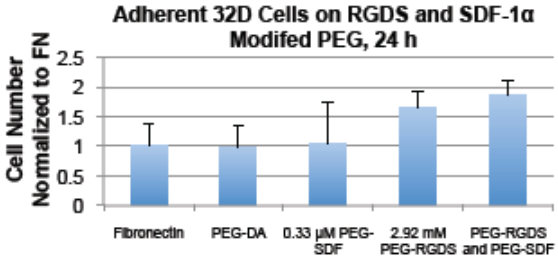

Figure 3: 32D Cell adhesion was increased on PEG gels modified with both SDF-1α and RGDS when compared to either biomolecule alone

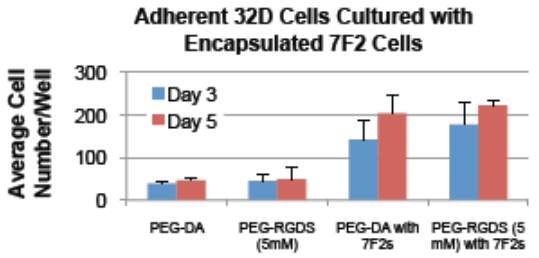

Figure 4: 32D Cell adhesion and proliferation was increased on PEG hydrogels containing 7F2 osteoblasts

References:

1. Wilson, A. Nat Rev Immunol, 2006; 6: 93-106.
2. Hahn, MS. Biomaterials, 2006; 27: 2519-2524.
3. Jones, LD. Nat. Rev. Immunol. 2008; 8: 290-301.

IMMOBILIZED PLATELET-DERIVED GROWTH FACTOR-BB PROMOTES ANGIOGENESIS IN POLY (ETHYLENE GLYCOL) BASED HYDROGELS

Jennifer E Saik[*], RA Poche[+], Emily Watkins[*], JE Barbick[*], ME Dickinson[+], and JL West[*].
*Rice University, Houston, TX +Baylor College of Medicine, Houston, TX
jsaik@rice.edu

Objective: The field of tissue engineering is severely limited by tissue engineered constructs' lack of microvascularization, which is necessary for transport of nutrients, oxygen, and waste. Platelet-derived growth factor BB (PDGF) is a key angiogenic protein able to support neovessel stabilization by inducing functional anastomoses and recruiting pericytes (1). Due to PDGF's widespread effects in the body and half life of only thirty minutes in circulating blood, local delivery and covalently immobilized PDGF may be necessary. Covalently immobilized PDGF was synthesized, and its bioactivity was confimed. PEGylated PDGF was then shown alone and in combination with PEGylated FGF in PEG-based hydrogels to induce HUVEC migration and tubulogenesis in 2D, 3D, and *in vivo* in the mouse cornea micropocket model (2).

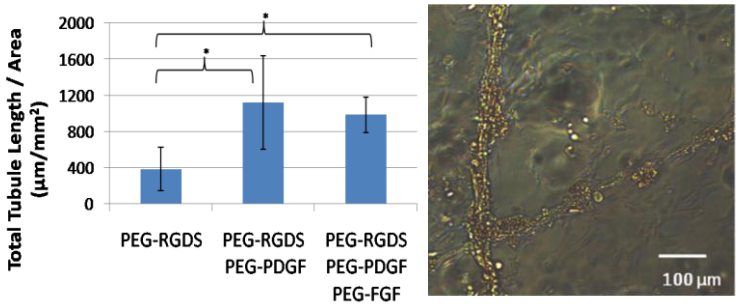

Figure 3: Total Tubule Formation on Modified Surfaces (*p<0.01)

Methods: PEG (MW = 6 kDa; Fluka, Milwaukee, WI) was acrylated by reaction with acryloyl chloride (3). PEG-succinimidyl carbonate-monoacrylate was reacted with RGDS in sodium bicarbonate buffer at a pH of 8.5 to form PEGylated RGDS. PEGylated basic fibroblast growth factor (FGF), PDGF, and vascular endothelial growth factor (VEGF) were made in a similar manner. 2D studies were performed by modifying the surface of a bulk PEGDA hydrogel as previously described (4) with a solution of 50 mg./mL PEG-RGDS, 17.6 µg/mL PEG-PDGF and/or 4.4 µg/mL PEG-FGF. HUVECs and/or 10T1/2 cells were seeded onto the modified gels and imaged using a fluorescent microscope. Cell-tracker labeled HUVECs were encapsulated into degradable hydrogels containing an MMP-sensitive peptide in the polymer backbone with 2µg/L PEG-PDGF and/or 0.5µg/L PEG-FGF and imaged over time on a confocal microscope. *In vivo* studies were performed by implanting a degradable hydrogel containing 320 ng VEGF per gel and 3.2 ng PEG-VEGF, or 320 ng PDGF, 3.2 ng PEG-PDGF, 80 ng FGF, and 0.8 ng PEG-FGF per gel into the cornea of *Flk1-myr::mCherry* transgenic mice as previously described (5).

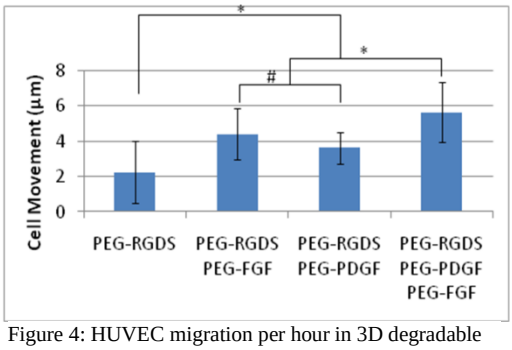

Figure 4: HUVEC migration per hour in 3D degradable hydrogels (*p < 0.01, #p <0.05).

Results: The bioactivity of PEG-PDGF was confirmed via increased 10T1/2 proliferation 48 hours after seeding cells on surfaces modified with PEG-RDGS and PEG-PDGF as compared to PEG-RGDS alone (p=0.015). HUVECs seeded on modified surfaces showed significantly more tubule formation on surfaces modified with growth factors as compared to surfaces modified with PEG-RGDS alone (p<0.01; Fig 1). HUVECs encapsulated into degradable hydrogels showed significantly higher migration in gels with covalently immobilized growth factors (p=0.01; Fig 2). In vivo vascular response to hydrogels incorporating both releasable and covalently immobilized PDGF-BB and bFGF (Fig 3 A-B), a previously established synergistic combination (6), showed a more robust vascular response than hydrogels with releasable and covalently immobilized VEGF (C-D). Furthermore, the different growth factors resulted in different vasculature morphologies, where hydrogels with PDGF and FGF induced larger diameter and more organized vessels.

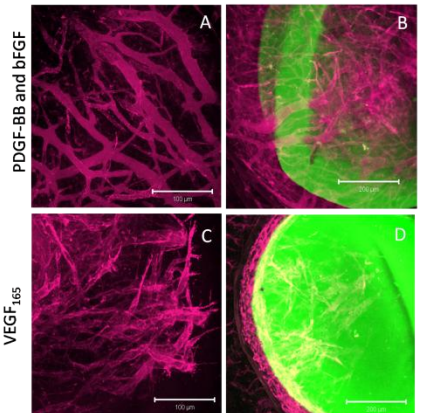

Figure 5: I*n vivo* vascular response to degradable hydrogels with both releasable and covalently immobilized factors.

Conclusions: Covalently immobilized PDGF promotes angiogenic activity, including endothelial cell migration and tubule formation. The *in vivo* vascular response in transgenic mice induces neovascularization, which can be regulated using rational design of bioactive hydrogels. Based on these results, bioactive hydrogels can be utilized to improve the formation of functional microvasculature for tissue engineering.

References:
1.Heldin CH. Physiol Rev. 1999 Oct;79(4):1283-316.
2.Rogers MS. Nat Protoc. 2007;2(10):2545-50.
3.DeLong SA. Biomaterials. 2005 Jun;26(16):3227-34.
4.Moon JJ. Biomacromolecules. 2007 Jan;8(1):42-9.
5.Poche RA. Dev Dyn. 2009 Sep;238(9):2318-26.
6.Cao R. Nat Med. 2003 May;9(5):604-13.

ENZYMATIC DEGRADATION OF POLY(LACTIC ACID) BASED NANOPARTICLES

†‡Samarajeewa, S.; ‡Li, Y.; ‡Murthy, K. S.; †‡Shrestha, R.; †‡Wooley, K. L.
†Texas A&M University, College Station, TX 77840
‡Washington University in St. Louis, St. Louis, MO 63130
sandani.samarajeewa@chem.tamu.edu, wooley@chem.tamu.edu

The construction of shell crosslinked knedel-like nanoparticles (SCKs) from enzymatically-degradable components is desirable for eventual biodegradability and for versatility in transformation of the nanoparticle materials, for instance excavation of the hydrophobic core domain to achieve higher encapsulation capacity of guest molecules. In this study, core-shell polymeric nanoparticles consisting of biodegradable poly(lactic acid) (PLA) core were prepared by supramolecular self assembly of amphiphilic block copolymer poly(lactic acid)-*b*-poly(*N*-(acryloyloxy)succinimide-*co*-(*N*-acryloylmorpholine)) in aqueous solution, followed by crosslinking of the hydrophilic shell region using amidation chemistry. Enzymatic degradation of the PLA core of micelles and SCKs was achieved upon the addition of proteinase K, a serine protease that exhibits high cleavage specificity at the peptide bond adjacent to the carboxylic groups of aliphatic and aromatic amino acids. The degradation behavior of PLA was monitored using nuclear magnetic resonance (NMR) spectroscopy and transmission electron microscopy (TEM). Kinetic analyses and comparison of the properties of the nanomaterials as a function of degradation extent will be presented. Hydrolysis of the PLA core and the subsequent extraction of small molecule degradation products generated entirely hydrophilic nanocages that have potential application in nanomedicine and other areas.

GASEOUS SENSITIZATION OF A HIGHLY EMISSIVE PHOSPHOR, K4[Pt2(P2O5H2)4].2H2O, FOR BIOLOGICAL APPLICATIONS

Nisa T. Satumtira1, Sreekar Marpu2, Oussama El-Bjeirami3, Purnima Neogi4, Turnbull Lon4, Vladimir Nesterov1, and Mohammad A. Omary1*

Departments of Chemistry1, Materials Sciences2, and Biology4

University of North Texas, Denton, Texas 76203

King Fahd University of Petroleum & Minerals3

Dhahran, Saudi Arabia

nisasatumtira@my.unt.edu

Objective: Aqueous solutions of K4[Pt2(P2O5H2)].2H2O (abbreviated "Pt-POP") exhibit strong green emission. When inert gases like N2 or Ar2 are introduced into the solution, the luminescence is enhanced. On the contrary, O2 tend to quench the emission. This interesting property compelled us to attempt introduction of Pt-POP into *in-vivo* models. The success of this study indicates cellular uptake of Pt-POP. Applications of this complex may expand to biological imaging applications.

Methods: Pt-POP was synthesized by microwaves using a modified version of a previously published method. Characterization included luminescence and absorption studies, as well as confirmation of structure by X-ray crystallography. Gaseous sensitization was studied by bubbling a solution with gas of choice of Pt-POP and measuring emission intensity at 515 nm. *In-vivo* studies were conducted using *E. coli* samples (strain DH5α). The bacteria were incubated with solutions of Pt-POP that were either deoxygenated or oxygenated. After incubation, the bacteria were evaluated using confocal microscopy. The resulting images gave indication of whether or not Pt-POP had been taken by the bacterium. 0 20 40 60 80 100 120 140 160 0 1x106 2x106 3x106 4x106 5x106 6x106 7x106 8x106 N2 N 2 O2 O 2 O2 Intensity

Results: The emission sensitivity of Pt-POP can be illustrated in the following figure. The peak maxima is a result of bubbling by N2, while peak minima is from the introduction of O2.

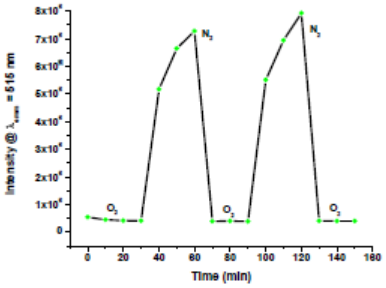

When introduced into *E.coli* cultures, the following images were collected via confocal microscopy:

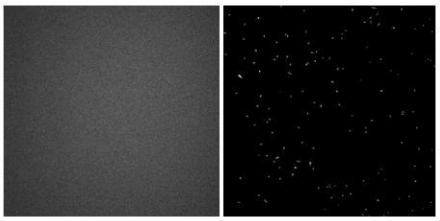

The image on the left is λexc = 405 nm at 64x magnification of *E.coli* bacteria itself, Upon incubation of the bacterium with Pt- POP, the image on the right is produced. Emission of Pt-POP is observed in the bacterium using λexc = 405 nm . Incubation of the bacterium in degassed solutions of Pt-POP produced enhanced intensity, similar to earlier solution studies.

Conclusions: A new synthetic technique for Pt-POP was developed. Aqueous solutions of Pt-POP were found to have emission enhancement when inert gases were introduced into the solution. Intensity decreased when O2 gas was used. Incubation of *E. coli* bacterium with Pt-POP showed successful uptake and retained emission of the metal complex by the organism. This was shown by confocal microscopy imaging. These results provide promising results for potential biomaterial applications in the future.

POLY(LACTIC-*CO*-GLYCOLIC ACID) MICROSPHERE-INCORPORATING POLY(METHYL METHACRYLATE) CONSTRUCTS FOR CRANIOFACIAL TISSUE ENGINEERING

Meng Shi,[1] James D. Kretlow,[1] Simon Young,[1,2] Mark E. Wong,[2] F. Kurtis Kasper,[1] Antonios G. Mikos[1,*]
[1]Department of Bioengineering, Rice University, Houston, TX USA
[2]Department of Oral and maxillofacial surgery, University of Texas Health Science Center at Houston, Houston, TX USA
*mikos@rice.edu

Objective: Craniofacial trauma is among the most debilitating forms of injury facing civilian and military populations due to the important aesthetic and functional role of the craniofacial complex. Blast injuries and injuries from high velocity projectiles (e.g., those encountered on the battlefield) often require a staged repair where the surgical revision, however, is sometimes complicated by distortion of surgical landmarks, diminished volume of the defect space, fibrosis of the tissue bed and/or local contamination. Over the course of a staged reconstruction, the placement of a temporary, alloplastic space maintainer may eliminate many of the aforementioned complications. Our laboratory is developing a novel regenerative medicine approach consisting of a first stage using temporary space maintenance to not only maintain the void space but also to prime the wound site for later definitive reconstruction using a regenerative medicine approach. The purpose of this study is to develop a functionalized porous poly(methyl methacrylate) (PMMA) construct as a space maintainer. A local antibiotic drug delivery system, poly(lactic-*co*-glycolic acid) (PLGA) microparticles loaded with colistin (a polymyxin antibiotic which was chosen specifically to address infections with *Acinetobacter* species, the most common pathogen associated with combat-related traumatic craniofacial injuries), was incorporated into the PMMA construct for treating/preventing local infections, potentially eliminating the infection-related complications associated with space maintenance.

Methods: Colistin-loaded PLGA (Mw 61 kDa, Lakeshore Biomaterials, Birmingham, AL) microspheres were fabricated by a water-in-oil-in-water double emulsion method. PLGA microsphere-incorporating PMMA constructs were fabricated by mixing a clinical grade bone cement formulation (SmartSet®, High Viscosity, DePuy Orthopaedics Inc., Warsaw, IN) of PMMA powder and MMA liquid with a carboxymethylcellulose (CMC) hydrogel to induce the surface/bulk porosity and colistin-loaded PLGA microspheres for drug release. Four formulations of PMMA/CMC/PLGA constructs with 40 or 50 wt% CMC and 10 or 15 wt% PLGA microsphere incorporation were investigated for surface and bulk morphology, handling characteristics during fabrication, porosity, pore interconnectivity by scanning electron microscopy (SEM) and microcomputed tomography (microCT) after fabrication and during a degradation process of 12 weeks. *In vitro* drug release kinetics were also examined over a period of 5 weeks.

Results and Discussion: CMC incorporation created controllable surface/bulk porosity and pore interconnectivity in the constructs. The porous structure is essential for successful space maintenance because a porous structure allows fibrovascular and other soft tissues to grow into the pores, promoting wound/tissue healing and the formation of a stable interface to anchor the implant in the host tissue. Colistin release, benefiting from the open paths created upon the CMC/PLGA dissolution, achieved a 5-week continuous release, potentially creating a local drug concentration well above the minimum inhibitory concentrations of colistin against susceptible species. Both the amount of drug release and the release duration meet the criteria of efficient local antibiotic delivery. The surface/bulk porosity, compressive mechanical properties, and *in vitro* drug release kinetics of the PMMA/CMC/PLGA constructs could be tuned by varying the weight percentages of CMC and PLGA incorporation, offering optimal opportunities to further refine the construct to match a specific clinical application in the two-stage regenerative medicine approach.

Conclusions: This study provides insights on the composition parameters that enable viable porosity characteristics/drug release kinetics of the PMMA/CMC/PLGA construct. Future investigation will focus on the evaluation of these PMMA/CMC/PLGA constructs in an infected craniofacial defect model for the role of surface/bulk porosity on the space maintenance capability and controlled drug delivery in treating local infections.

STUDY OF DIFFERENT ETCHING PROCESSES FOR REMOVAL OF RESIDUAL MEMBRANES OF OPEN CELL SHAPE MEMORY POLYMER FOAMS

Singhal, P., Wilson, T. S., Maitland, D. J.
Texas A&M University, College Station, TX; Lawrence Livermore National Laboratories, Livermore, CA
pooja52k2@yahoo.com

Objective: Objective is to study different protocols for effectively removing cell membranes from the partially open celled shape memory polymer foams and form completely open cell structures. It is hypothesized that flow based etching removes the weakly linked residual membranes and sonication, combined with acidic environment developed by the hydrochloric acid, assists in the clean cleavage of membranes. The effect that this process has on the shape memory behavior and other physical properties of this material has been studied to confirm any changes in other physical properties.

Methods: Shape memory foams were synthesized via blowing process using Hexamethylene Diisocyanate (TCI America), Tri-Ethanol Amine (TCI America), Hydroxyl Propyl Ethylene Diamine (TCI America) as base reagents. Samples were cleaned by following methods:

I. Static etching in 0.01 N Hydrochloric acid for 6 hours at 30°C
II. Sonication with static etching in 0.01N Hydrochloric acid for 6 hours at 30°C
III. Flow etching (using an in-house developed flow assembly) in 0.01 N Hydrochloric acid for 6 hours at 35 ml/min at 30°C
IV. Sonication with flow etching in 0.01 Hydrochloric acid for 6 hours at 35ml/min at 30°C
V. Directed flow etching in 0.01 N Hydrochloric acid for 1.5 hrs at 30 °C, with increased flow (70 ml/min) on the sample and sonication.

Any changes in weight and hence density of the samples were measured after the cleaning. Also glass transition and shape memory behavior were recorded before and after the cleaning process. Cell structure of the foam was studied at the same spot of foam before and after the cleaning procedures using scanning electron microscopy.

Results: Static conditions were found to be more damaging to the cell structure compared to flow based etching. Supplying sonic energy was seen to direct the etching better to the weaker membranous areas due to vibration, resulting in complete membrane removal and cleaner cut edges. The results were supported by the physical properties of the treated samples. Better membrane removal of flow based cleaning showed retention of shape memory behavior, lower net mass loss and higher transition temperature due to more effective removal of plasticizing agents.

Conclusions: A combination of sonication and flow based etching in mildly acidic environment can provide better removal of residual membranes in open cell foam structure.

TRI-FUNCTIONAL THERANOSTIC SILICA NANOPARTICLES FOR IMAGING, DELIVERY AND BIOMATERIAL REINFORCEMENT

[a,b]Christine Smid, [a,b]Rachel Buchanan, [a]Nicoletta Quattrocchi, [a]Iman Yazdi, [c]Diana Yoon, [c]Kurt Kasper, [c]Antonios Mikos, [d]Brad Weiner, [a,b]Mauro Ferrari, [a]Ennio Tasciotti
[a]Department of Nanomedicine Biomedical Engineering
University of Texas, Health Science Center, Houston Texas
[b]Department of Biomedical Engineering
University of Texas, Austin Texas
[c]Rice University, Houston Texas
[d]The Methodist Hospital, Houston Texas
e-mail: Christine.Smid@uth.tmc.edu

Objective: In this work we developed Theranostic Silica Nanoparticles (TSNs) for drug delivery, cellular and tissue targeting and in vivo imaging. The ability to control pore size, particle size, surface area, porous framework and pore volume, enables the tuning of the TSNs to their desired applications. Biodegradability together with the absence of any cytotoxic effect make TSNs a versatile solution for the delivery of drugs, genes, siRNAs and contrast agents. Through appropriate surface functionalization the TSNs were directed towards subcellular localizations (figure 1A) or incorporated into polymeric scaffolds as nanoreinforcement.

Methods and Results: 25-50nm TSNs (figure 1B) were used to show the controlled release of Doxorubicin, growth factors and antibiotics. DNA and siRNA were conjugated for gene therapy and gene silencing. By tuning various parameters within the TSN synthesis, each chemical and physical parameter of the system was finely tuned to obtain specific release kinetics. Also through the conjugation of short peptides sequences, subcellular targeting was accomplished.
Additional modifications of the TSNs were developed and characterized to: i) promote dispersion in physiological conditions; ii) allow for their tracking and localization; iii) incorporation into the silicon multistage delivery system recently developed by our group [1, 2].
Finally, due to the biomechanical properties of porous silica, TSNs can be used as mechanical reinforcement of polymeric composite materials for orthopedic applications. By varying the reagent ratios, we synthesized TSNs with different morphologies and aspect ratios (figure 1B,C). This together with the appropriate surface modification enabled the stable incorporation of the TSNs into polymeric matrices and increased the mechanical properties of the material.

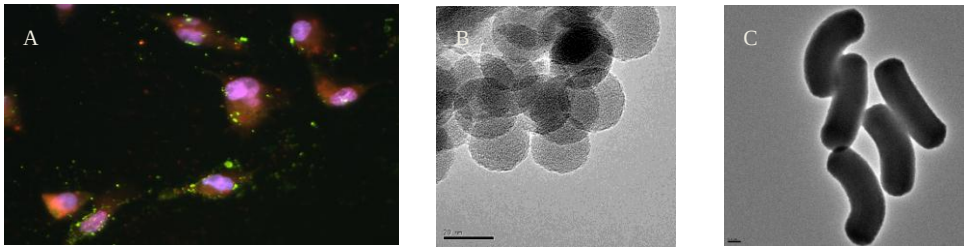

Figure 1A. Fluorescence Microscopy image of silica loaded with DOX internalization (blue stains cell nuclei, red stains for DOX loaded inside silica nanoparticles, and green stains the PS indicative of early stage apoptosis). Figure IB. Uniform size distribution of silica nanoparticles loaded with DOX-HCL during fabrication. Figure 1C Silica nanoparticles with higher aspect ratio for mechanical reinforcement.

References:

[1] Tasciotti, E., et all, *Nat. Nanotechnol.*, 2008, vol. 3 (3): 151-7
[2] Serda R.E. et al. Biomaterials, 2009, vol 30c(13): p. 2440-8.

COMPARISON OF BANDAGES COATED WITH ORGANO-SELENIUM OR SILVER FOR THEIR ABILITY TO INHIBIT BACTERIAL ATTACHMENT

Phat Tran[1], Thomas Mosley[2], Mayank Shashtri[3], Janette Cortez[1], Abdul Hamood[1], Ted W. Reid[1,2],
Texas Tech University Health Sciences Center[1], Selenium Ltd.[2], Eburon Organics International[3]
Phat.Tran@ttuhsc.edu

Objectives: It has been found that selenium can be covalently attached to an organic molecule while still retaining its ability to catalyze the formation of superoxide radicals ($O_2^{-\cdot}$) from the oxidation of thiols. This selenium chemistry is seen in the following equation:

$$R\text{-}Se^- + 2O_2 + 2\ R'\text{-}S\text{-}H \rightarrow R\text{-}Se^- + 2O_2^{-\cdot} + R'\text{-}S\text{-}S\text{-}R'$$

The purpose of this study was to test whether it was possible to modify the surface of cellulose bandages, with an organo-selenium coating, so as to block the ability of bacteria to attach to the bandage and form a biofilm and to compare this material with a commercial silver coated bandage. The bandages were also tested to see if they released any toxic material that might harm mammalian cells.

Methods: Selenium was covalently attached to a methacrylate. This organoselenium methacrylate was then mixed with different amounts of the methacrylate that didn't contain selenium and then was attached as a coating to the surface of a cellulose bandage. The selenium-bandage was then placed over a selenium-free bandage that was inoculated with bacteria (*Staphylococcus aureus* or *Pseudomonas aeruginosa*) in a nutrient media. This was placed on an agar plate in a moist chamber at 37 degrees. After 24 hours growth in the nutrient media, the number of bacteria that attached to the selenium-bandage (colony forming units, CFU) was determined. Bacterial attachment was also evaluated by scanning electron microscopy (SEM). A dose response study to determine the amount of selenium necessary to inhibit bacterial attachment was performed by adding methacrylate containing different amounts of selenium. Toxicology studies were also performed with mammalian cells where the selenium-coated bandage was soaked for a week in the media. This media was then tested for toxicity to the mammalian cells. This assay was modified for comparison with the commercially available silver coated bandages. Soft agar was mixed with 10^8 *Staphylococcus aureus* 31 bacteria and then poured on an LB agar plate. The bandage material (selenium or silver coated; 1 cm sq) was placed on top of the soft agar plate. This was incubated for 16 hours at 37^{o}C. The bandage was then removed and placed in 1 ml of PBS at pH 7.4. This material was then was vortexed and CFUs were determined.

Results: From dose response studies it was determined that a concentration of 0.2% selenium (55ug Se/sq cm) in the coating was sufficient to block 100% of the *S. aureus* bacterial attachment as determined by CFU. Ninety five% inhibition was seen at 0.05% selenium (l3 ug Se/sq cm). This was in the presence of over $l0^8$ bacteria. SEM studies confirmed these results. No toxicity to mammalian cells was observed from the solution obtained by soaking of the selenium-coated bandage. In comparison experiments, the selenium-coated bandage showed complete inhibition of over 10^8 *Staphylococcus aureus* 31 bacterial attachment, the silver coated bandage only showed 1 to 2 logs of inhibition

Conclusions: Selenium can be covalently attached to a cellulose bandage material by a simple dip coating process and still retain its ability to catalyze the formation of superoxide radicals. Selenium covalently attached to a coating on a bandage has the ability to completely inhibit the attachment of 8 logs of both gram negative and gram positive bacteria (as seen by CFU and SEM assays) with no toxicity towards mammalian cells. A commercially available silver coated bandage only showed 1 to 2 logs of inhibition.

SYNTHESIS OF CELL-RESPONSIVE, BIODEGRADABLE POLYUREAS FOR LIGAMENT TISSUE ENGINEERING

Turner, P A; Benhardt, H A; Cosgriff-Hernandez, E
Texas A&M University, College Station, TX
Pat006@neo.tamu.edu

Objective: Anterior cruciate ligament (ACL) injuries are a significant clinical problem, resulting in 200,000 reconstructive surgeries in 2002 and incurring a cost in excess of 5 billion dollars [1,2]. A synthetic ACL graft should possess sufficient mechanical properties to restore ligament function while degrading at a rate complementary to tissue regeneration. This synergistic relationship insures that mechanical integrity is maintained throughout the healing process, while preventing stress shielding or premature overloading of the new tissue. Segmented block polyureas are excellent candidates for ligament tissue engineering because of their biocompatibility, versatility, and favorable mechanical properties, which may be tailored by altering their composition such as the soft to hard segment molecular weights and chemistries and hard segment: soft segment weight ratio. Incorporation of a collagen-derived peptide sequence can render the polymer responsive to cell activity, particularly enzyme-mediated degradation associated with ligament tissue remodeling. This design allows superior coordination of tissue regeneration and scaffold degradation over currently used synthetic polyurethanes, which degrade principally by non-specific hydrolysis. A library of cell-responsive polyureas was synthesized from peptide-polyether soft segments and aliphatic hexane diisocyanate (HDI) and ethylene diamine (ED) hard segments. Soft segments were synthesized using poly(ethylene glycol) (PEG, Fluka Chemical), mw 1000 and 2000 g/mol, and poly(tetramethylene) glycol (PTMG, Polysciences Inc.), mw 1000 g/mol. A biodegradable peptide sequence (GPQGIWGQGK), provided by Baylor Protein Chemistry Core Laboratory, was then incorporated into the soft segments. These soft segments were then reacted with isocyanate and diamine chain extenders to produce biodegradable, cell-responsive polyureas with variable soft segment chemistries and hard segment composition.

Methods: Coupling the peptide sequence with the soft segment polyols requires favorable end-group matching. PEG and PTMG were first reacted with succinic anhydride to yield carboxylic acid end groups [3]. The acid-functionalized polyols were then reacted with N-hydroxysuccinimide (NHS) to give end groups favorable for peptide bonding. The polyols were then bound to peptide sequences, forming a peptide-polyol-peptide triblock [4], which was then further reacted with more of the NHS-functionalized polyol to yield the complete soft segment multiblock. End-group functionalization and percent yield were measured at each step using FTIR and NMR, respectively. Higher molecular weight PEG (6000, 10000 g/mol, Fluka Chemical) and PTMG (2900 g/mol, Polysciences Inc.) were functionalized with amine groups and used as control soft segments in polyurea synthesis. Amine functionalization was confirmed with Ninhydrin assay. Following multiblock synthesis and amine functionalization, polyureas were produced by reacting the soft segment multiblocks with HDI and ED. Two ratios of HDI to soft segment to chain extender were chosen (5:1:4 and 3:1:2) to investigate the effect of hard segment: soft segment ratio on mechanical properties of the synthesized polyureas, resulting in hard segment weight fractions ranging from 6-17%.

Results: FTIR confirmed the acid-funcionalization of all polyols, showing increased absorption due to ester formation at 1730 cm^{-1} relative to an internal reference ether peak, with less pronounced absorption at higher molecular weights. Analysis of NHS-functionalized compounds revealed a similar trend, with increased absorption at 1730 cm^{-1} due to NHS-ester formation. ^{1}H-NMR also indicated at least 90% functionalization of all polyols following carboxylic acid coupling, with appropriate peak shifting observed following NHS bonding. Amine functionalization was confirmed by FTIR, with absorbance peaks observed at 1658 cm^{-1} due to amide formation, with a corresponding decrease in absorbance at 1730 cm^{-1} due to loss of ester groups. Positive Ninhydrin assay confirmed the presence of free amine groups. Successful formation of the peptide-polyol-peptide triblock was confirmed with FTIR based on the formation of amide peaks at 1660 cm^{-1}, indicative of the peptide backbone, and decrease at 1730 cm^{-1} due to loss of ester groups. Peaks in NMR spectra at 7.1-8.2 ppm and positive Ninhydrin assay confirmed successful peptide-polyol coupling. Polyurea formation was confirmed with FTIR, showing absorbance peaks at 1632 cm^{-1} (C=O) and 3320 cm^{-1} (N-H).

Conclusions: Incorporation of cell-responsive peptides into the design of novel biomaterials provides a useful mechanism for modulating their degradation *in vivo*. The results of this study indicate the successful synthesis of segmented block poly(ether ureas) whose degradation is modulated by cell activity and mechanical properties may be altered by changing the segment composition and ratios. The next step will be to characterize these polymers, particularly to quantify the structure property relationships associated with soft segment chemistry and hard segment: soft segment weight ratio. Finally, the effect of polymer chemistry and influence of the peptide sequence on enzyme-mediated degradation may be investigated. The results of this study may be applied to design of a material with mechanical and degradation properties tailored for ACL reconstruction.

References:

[1] Albright JC. Am Acad Ortho Surg. 1999.
[2] Pennisi E. Science. 2002; 295, 1011.
[3] Ma XJ. Biomed Mater Res. 1993; 27: 357-365
[4] West JL. Macromolecules. 1999; 32: 241-244.

THREE-DIMENSIONAL, FINITE ELEMENT MODELING OF SHAPE MEMORY POLYMERS

Volk, B L; Lagoudas, D C; Maitland, D J
Texas A&M University, College Station, TX
brentvolk@tamu.edu

Objective: The objective of this work is to present the three-dimensional modeling efforts of shape memory polymers.

Methods: This work will focus on the three-dimensional numerical implementation of a finite deformation constitutive model. This previously developed model is based on the theory of nonlinear thermoelasticity, and accounts for the coexisting active and frozen phases of the SMPs as well as the transition between the two phases. The model is implemented as a user material subroutine (UMAT) in ABAQUS.
The material properties in the model are calibrated from finite deformation experimental data of polyurethane (PU) SMPs. Tensile tests are performed on the PU specimens for both constant strain and constant stress recovery scenarios. After calibrating from a subset of the experimental results, the model is used to predict the material response for the other thermomechanical load paths.

Results: The implementation of the constitutive model results in the first attempts at modeling the large deformation response of biomedical applications, such as cardiovascular stents, which incorporate shape memory polymers.

Conclusions: This work provides a valuable analysis tool for the design and optimization of biomedical devices through allowing a prediction of the material response, including the development of stress concentrations and the maximum recoverable deformations. Future efforts will consider irrecoverable deformations, heat transfer, and viscoelastic and viscoplastic phenomena.

STUDY OF AMYLOID-BETA (AB) FIBRILLIZATION USING QCM

Jinghui Wang
Rice University

Alzheimer's disease (AD) is the most common neurodegenerative disease affecting today more than 4.5 million people in the US alone. The hallmark of the diseases is the deposition of Aβ peptide into amyloidogenic fibrils. However, recent evidence shows that the prefibrillar forms of Aβ are the folding species responsible for cellular toxicity, whereas the insoluble deposits are a means for the cell to localize these toxic misfolded species into a separate cellular compartment and avoid deleterious interactions. The purpose of this study is to characterize and understand the process of Aβ peptide fibrillization using quartz crystal microbalance (QCM). QCM measures mass change per unit area by measuring the change in frequency of a quartz crystal resonator. Frequency measurements are translated into precise mass changes. We are also able to measure the changes in the elastic properties of the film by monitoring its dissipation. Using these two signals, we can monitor fibril attachment and nucleation on a surface. Aβ fibrillization is also monitored in this study using fluorescence-based under various experimental condition for comparison.

PROBING THE MECHANICAL PROPERTIES OF PLASMA VON WILLEBRAND FACTOR USING ATOMIC FORCE MICROSCOPY

+*Wijeratne, S; *Botello, E; *Frey, E; **Dong, J-F; **Yeh, H-C; *Kiang, C-H
*Rice University, Houston, TX
** Baylor College of Medicine, Houston, TX
+ssw6@rice.edu

Single-molecule manipulation allows us study the real time kinetics of many complex cellular processes. The mechanochemistry of different forms of von Willebrand factor (VWF) and their receptor-ligand binding kinetics can be unraveled by atomic force microscopy (AFM). Since plasma VWF can be activated upon shear, the structural and functional properties of VWF are critical in mediating thrombus formation become important. Here we characterized the mechanical resistance to domain unfolding of VWF to determine the conformational states of VWF. We found the shear induced conformational, hence mechanical property changes can be detected by the change in unfolding forces. The relaxation rate of such effect is much longed than expected. This supports the model of lateral association VWF under shear stress. Our results offer an insight in establishing strategies for regulating VWF adhesion activity, increasing our understanding of surface-induced thrombosis as mediated by VWF.

SHAPE MEMORY FOAMS BASED ON SILICON-CONTAINING POLYMERS

+*Zhang, D.; Weyand, C.B.; Grunlan, M.A.
+Texas A&M University, Department of Biomedical Engineering, College Station, TX
zhangdavei@neo.tamu.edu

Objective: Shape memory polymers (SMPs) are stimuli-responsive materials which change their shape upon application of an external stimulus such as heat.[1] SMPs based on both physically and chemically crosslinked poly(ε-caprolactone) (PCL; T_g = -60 °C) have received much attention due to PCL's biodegradability and elasticity. We have recently reported "hybrid" inorganic-organic SMPs prepared via the photochemical cure of a series of photosensitive triblock macromers consisting of a central inorganic polydimethylsiloxane (PDMS) segment and terminal organic PCL segments of varying lengths (Figure 1).[2] In this system, the PCL served as the switching segment and PDMS served as the soft segment to tailor mechanical properties. As PCL segment length increased and hence crosslink density decreased, an unusual simultaneous increase of *%ε* (strain at break), *E* (elastic modulus) and *TS* (tensile strength) was observed. In this present work, the corresponding *SMP foams* were fabricated from these macromers using a poragen-leaching technique. SMP foams are of interest as the thermal actuating properties of SMPs can be enhanced by their structuring into low-density open foam cells. In addition to shape fixity and recovery, SMP foams offer increased surface area, compressibility, energy absorption and heat insulting properties. Many potential applications have focused on the aerospace field (e.g. space deployable support structures, shelters for space habitation, and rover components) and biomedical fields (e.g. aneurysm treatment – "embolic sponges"). Previous studies on SMP foams have been largely limited to those based on polyurethanes and epoxies.[3,4] Thus, the lack of SMP foams having Si-containing polymer components motivated this research.

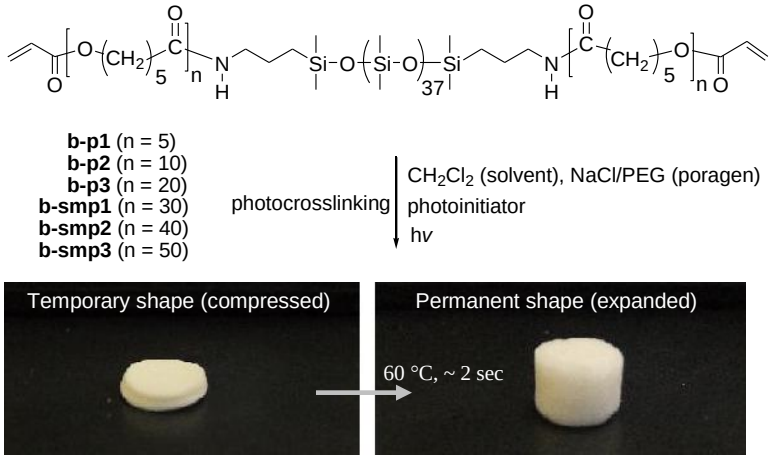

Figure 1. AcO-PCL$_n$-*block*-PDMS$_{37}$-*block*-OAc macromers and their photochemical cure to form SMP foams with a poragen leaching technique.

Methods: Photo-sensitive macromers AcO-PCL$_n$-*block*-PDMS$_{37}$-*block*-PCL$_n$-OAc were synthesized as previously reported.[2] SMP foams were fabricated with a poragen leaching method.[5] Monomethoxy-terminated polyethylene glycol (PEG) (2k g/mol) served as a suspension agent in which NaCl salts (< 250μm) could become uniformly dispersed. After dissolving the macromer in dichloromethane (DCM) in a glass vial, PEG, NaCl, and photoinitiator solution were sequentially added with additional vortexing. To each 1 mL of mixture solution was added 150 μL of photocatalyst solution [10 wt% solution of 2,2-dimethoxy-2-phenyl-acetophenone (DMAP) in 1-vinyl-2-pyrrolidinone (NVP)]. The resulting precursor mixture was exposed to UV light (UV-Transilluminator, 6 mW/cm^2, 365 nm) for 3 min. After air drying for 24 h, the resulting foam plugs were soaked in DI water on a shaker table for 4 days to remove the PEG and NaCl and dried *in vacuo* (36" Hg, 80 °C, 4 h).

Results and Conclusions:
By systematically varying macromer concentration, NaCl/PEG ratio and annealing temperature during final vacuum drying, foam density, porosity, and mechanical properties were varied. Shape memory tests revealed that these foams can reduce their size by 200% by collapsing porous domains and recover to original dimensions upon heating. We will examine pore structure via SEM imaging in future work. PDMS-PCL SMP foams whose properties may be altered by changing fabrication variables are of interest to produce property-specific materials for a particular application.

References:
1. Lendlein, A.; Kelch, S. *Angew. Chem. Int. Ed.*, 2002, **41**, 2034-2057.
2. Schoener, C.A.; Weyand, C.B.; Murthy, R.; Grunlan, M.A. *J. Mater. Chem. accepted.*
3. Ortega, J.; Maitland, D.; Wilson, T.; Tsai, W.; Savas, O.; Saloner, D. *J. Biomed. Eng.* **2007,** 35, 1870-1884.
4. Prima, M. A. D.; Lesniewski, M.; Gall, K.; McDowell, D. L.; Sanderson, T.; Campbell, D. *Smart Mater. Struct.* **2007,** 16, 2330-2340.
5. Courtois, J.; Bystrom, E.; Irgum, K. *Polymer* **2006,** 47, 2603-2611.